

# Instrumentation and diagnostics

M. Marchevsky, LBNL

Credits to: D. Arbelaez, M. Turqueti, R. Teyber, E. Hershkowitz, T. Shen, K. Zhang, X. Wang, P. Bish, J. Swanson, S. Gourlay, S. Prestemon and all members of the Superconducting Magnet Group and Diagnostics Workgroup of MDP

# Goals of magnet diagnostics

## General and predictive

- **Understanding training and memory effects in magnets through disturbance spectrum analysis**
- Finding weak spots and design limitations and feeding back to magnet designers
- Benchmarking of models on stress, internal voltages, protection, ac losses, etc.



**Improving performance**

## Operational

- **Quench detection**
- **Quench locations and NZPV**
- **Flux jumps and conductor instabilities**
- **Mechanical stability monitoring**

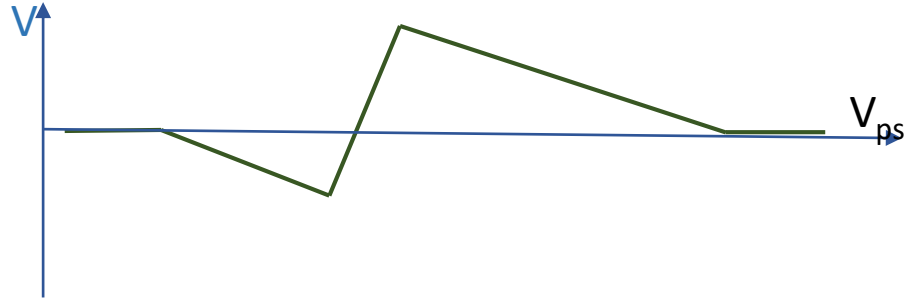


**Detecting problems, preventing damage**



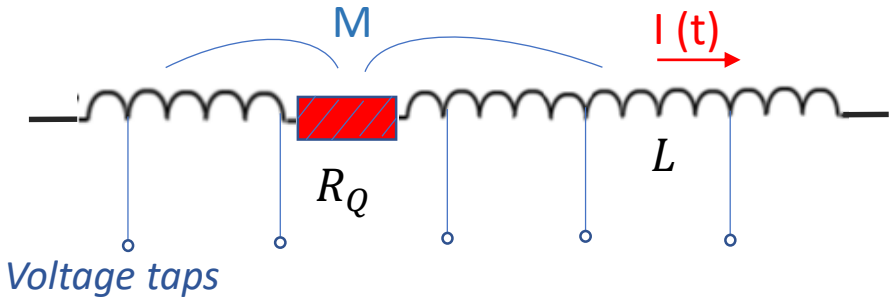
# Voltage diagnostics

# Voltage detection: the “traditional” technique



$$V_Q(t) = I(t)R_Q(t) - M \frac{dI(t)}{dt}$$

$$L \frac{dI(t)}{dt} \cong I(t)R_Q(t)$$



$$V_Q(t) = I(t)R_Q(t) \left(1 - \frac{M}{L}\right)$$

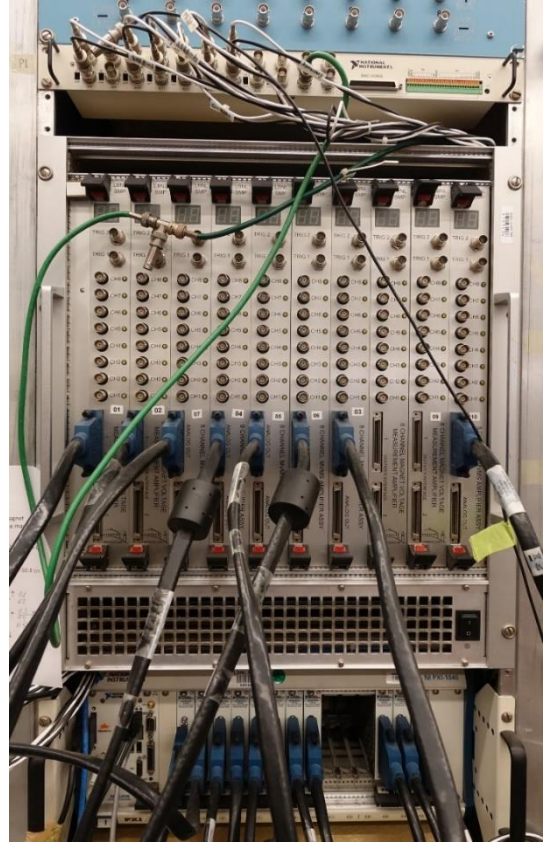
$V_Q(0) = V_Q(\infty) = 0 \Rightarrow$  peaks during the quench



Voltage taps examples

## “Magnet Voltage Measurement System” (MVMS)

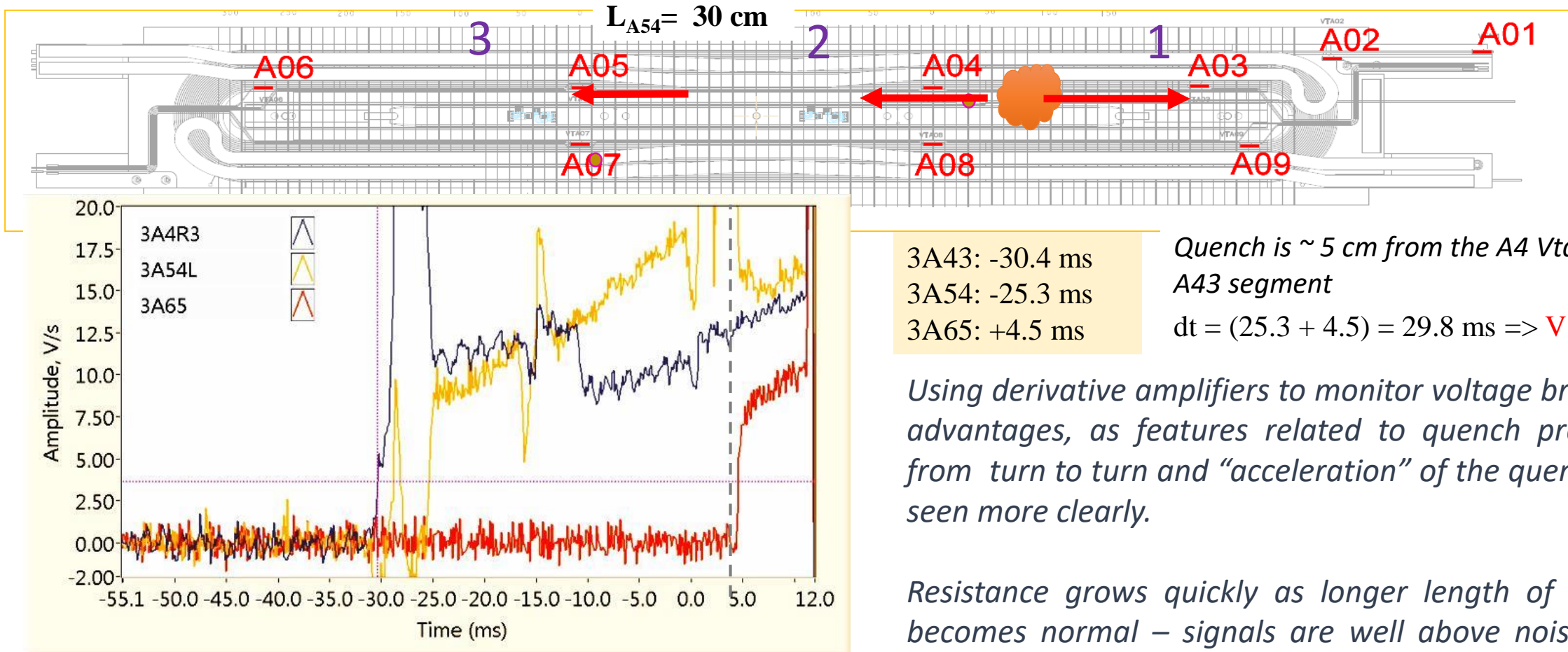
- 160+ DAQ channels at 500 kHz
- National Instruments PXI-6123 cards interfaced to remotely programmable custom built HV (1000 V to ground) buffer amplifiers



Internal magnet voltage during quench may reach several hundreds of volts!

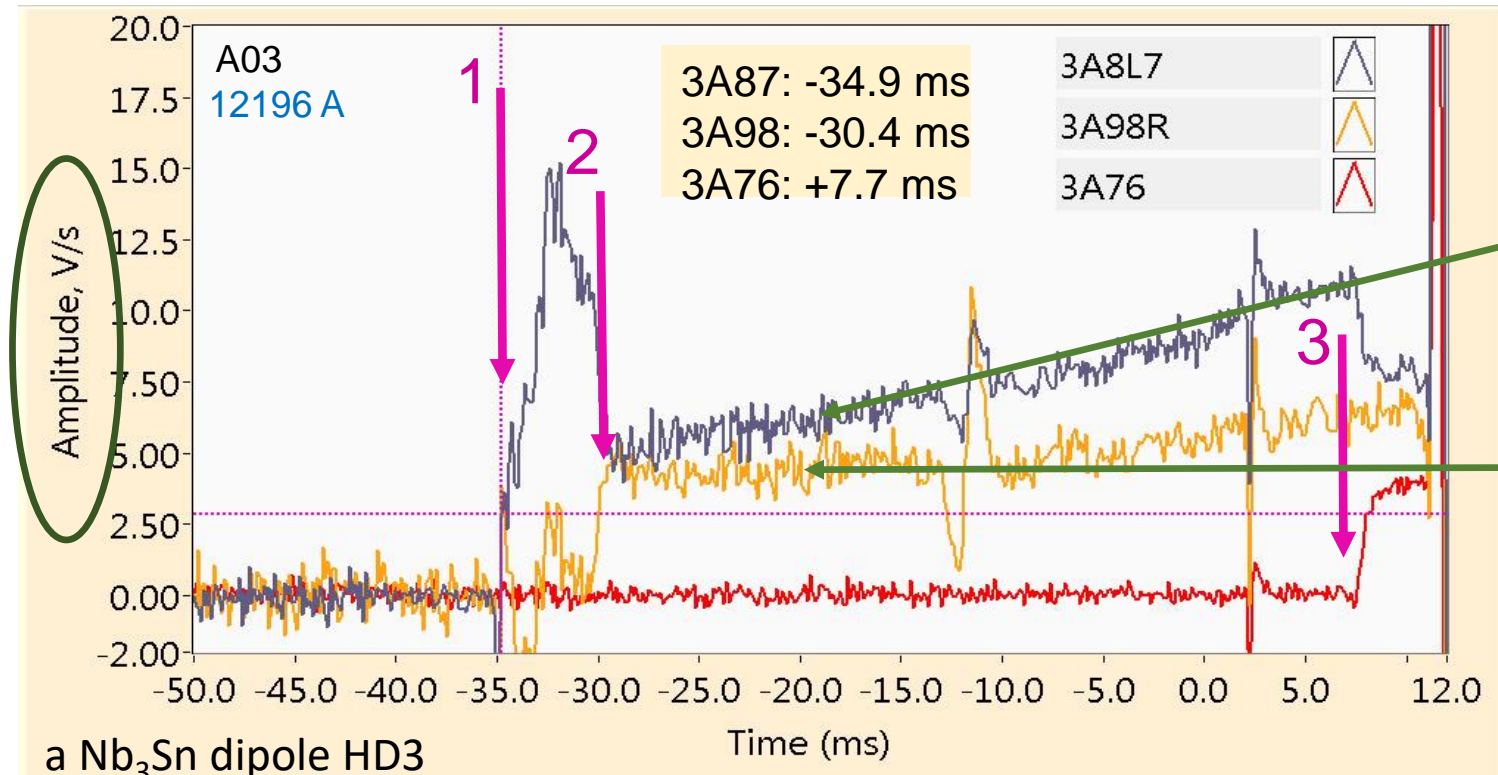
# Example of voltage-based quench localization in HD3 dipole

Voltage acquisition is typically triggered by the QD system and most useful quench data are collected in a short (5-40 ms typical) time window prior to a current extraction.



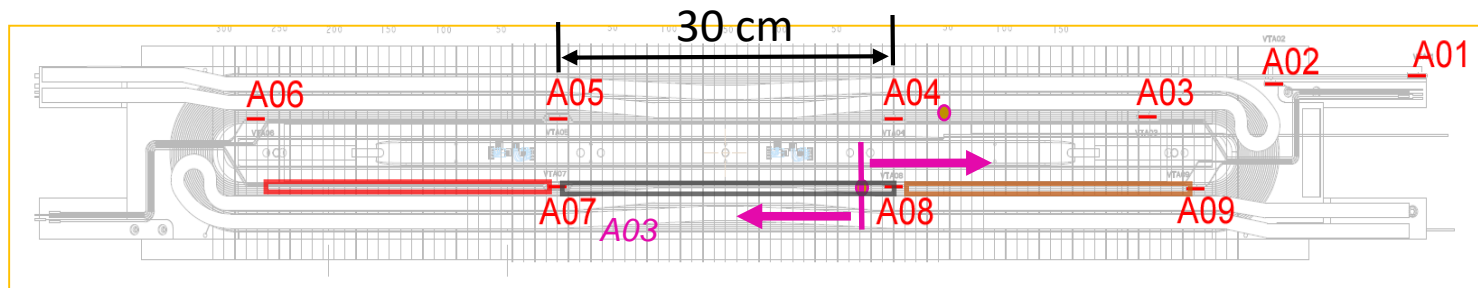
Test of Nb3SN high field dipole HD3 at LBNL

# Another HD3 example



Acquisition is triggered by the quench detection system (trigger arrives at time "0")  
Accelerated propagation

Steady propagation



Quench starts ~ 3 cm from the A8 Vtap in the A87 segment segment

$$L_{A87} = 30 \text{ cm};$$

$$dt = (4.5 + 42.6) = 47.1 \text{ ms}$$

$$\Rightarrow V = 6.3 \text{ m/s}$$

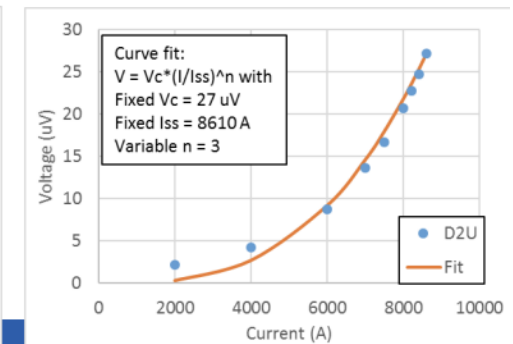
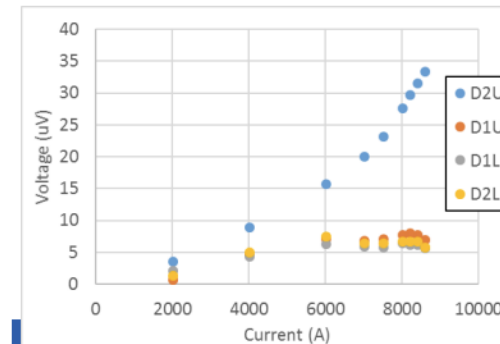
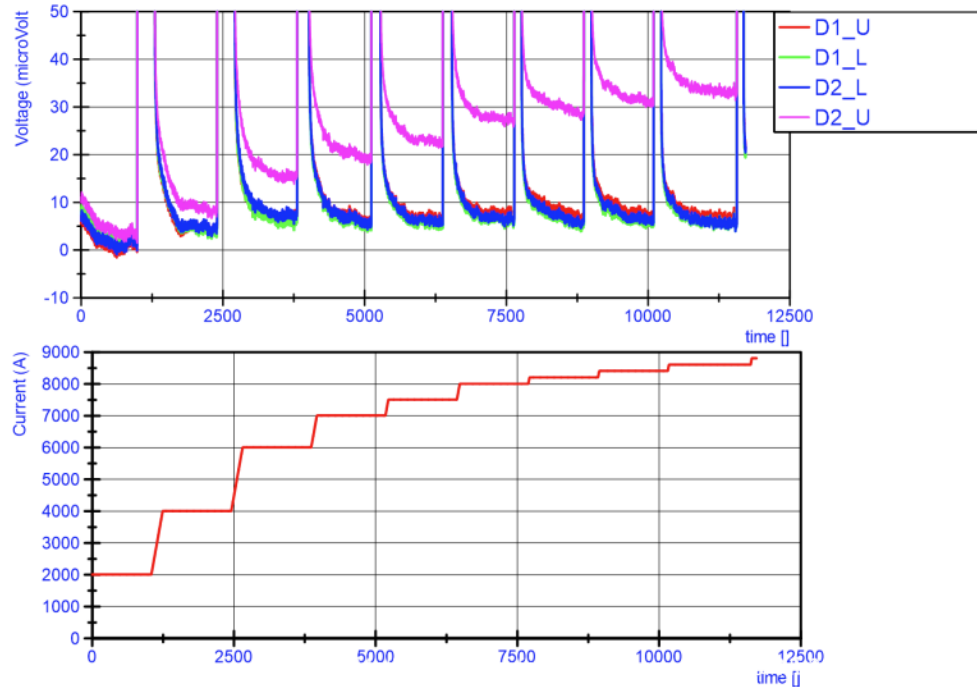
# Low-level voltage measurements reveal conductor degradation

Challenge: Voltage measured over full 5.5 meter 56 turn coils (600 meter of cable)  
 Large effects of inductance and decay effects after each ramp!

Solution: Increase plateau duration to 20 minutes (3h measurement)  
 & compare 4 coils measurements

1 coil is clearly showing a resistive voltage buildup, of up to 30  $\mu\text{V}$  at 8.8 kA.  
 The V-I curve, see below, can be fitted with linear curve, rather than the expected high n-value.

It proves a clear conductor degradation already showing at low current.

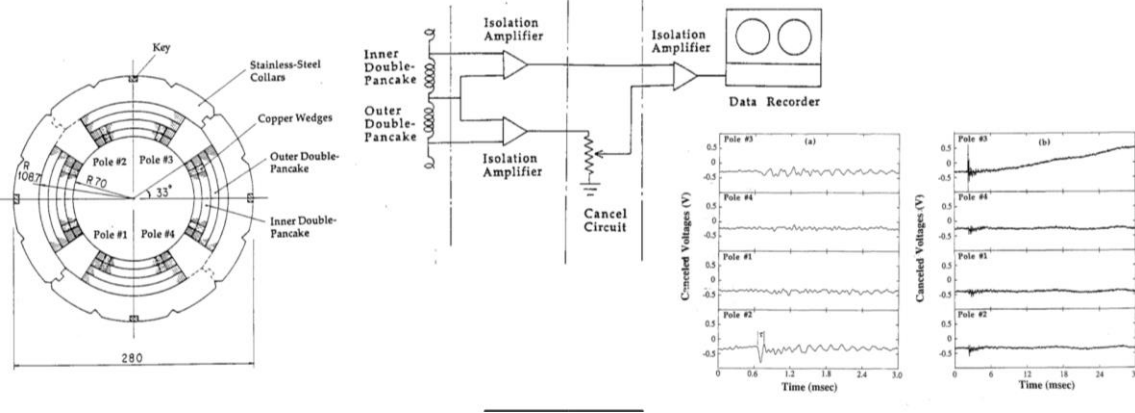


magnets used at CERN, Willering, IDSM 01, Berkeley, 24 April 2019

# Detecting disturbances

Wire motion search in late 1980 to early 1990

- Investigation of wire motion in superconducting magnets, T. Ogitsu, K. Tsuchiya, A. Devred 1991



Voltage taps can be monitored to detect conductor motion or an electromagnetic instability (flux jumps) during magnet ramping and operation, providing an insight on quench causes or conductor damage

If the monitored conductor segment is long (= high inductance), fast fluctuation will be “filtered out”.

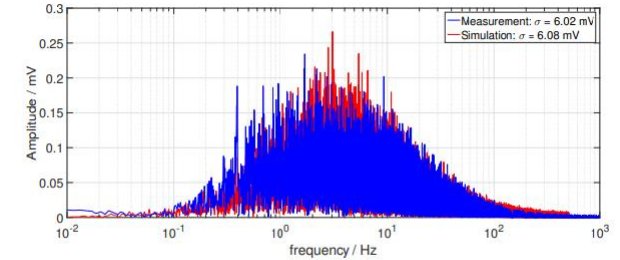
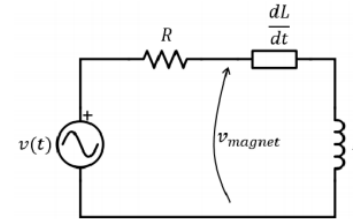
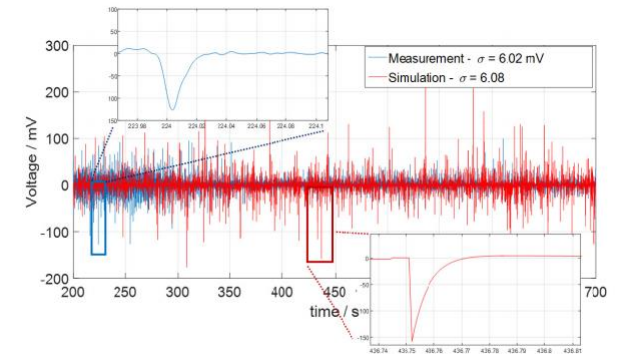


Figure 6. Simulation and measurement results in frequency domain.

“Impact of Flux Jumps on High-Precision Powering of Nb3 Sn Superconducting Magnets”, M. Martino et al 2019 J. Phys.: Conf. Ser. 1350 012180





# Advantages vs disadvantages of Vtaps

Voltage taps are still a very useful and versatile diagnostic tool. Besides providing input to the QD system, they also allow to measure (in certain cases) a quench origin location, quench propagation velocity, as well as to learn about some finer details of quench propagation dynamics.

Key disadvantage, however, is that voltage taps are invasive and have to be built into the magnet during fabrication. Some magnets (like those installed in the accelerator or those to be used in fusion machines, for instance) aim at avoiding them completely.

Accuracy of quench localization is only as good as the density of Vtaps

Voltages are much lower in HTS magnets because NZPV is 1-2 orders of magnitude lower in HTS... (cm/s vs m/s in LTS). This implies that voltages to be detected are  $\sim 1$  mV or lower and this becomes challenging for large magnets especially where currents is ramped (accelerators) or a strong EM background is present (fusion). Hence, alternative QD techniques are being explored for HTS.



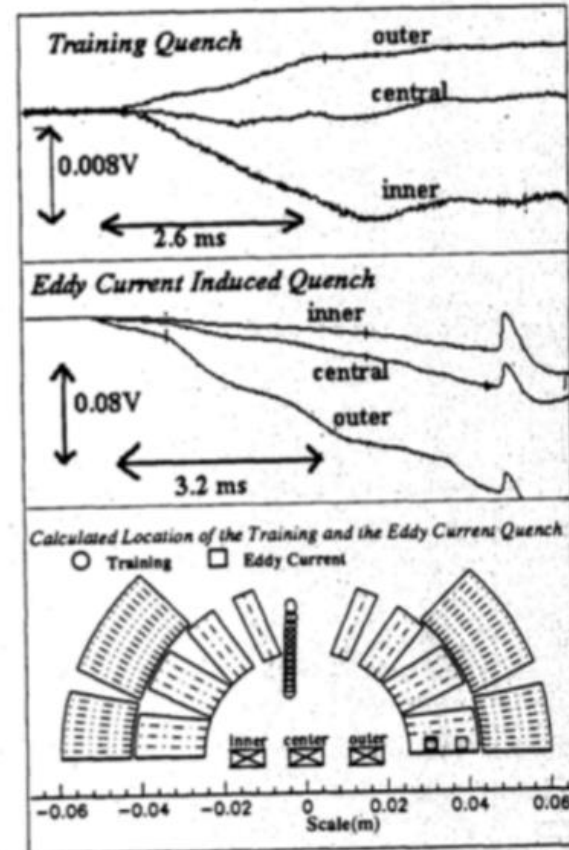
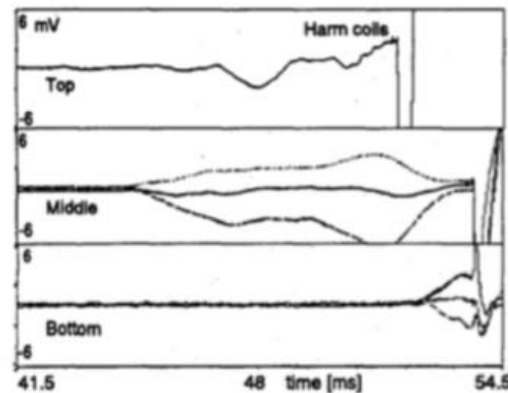
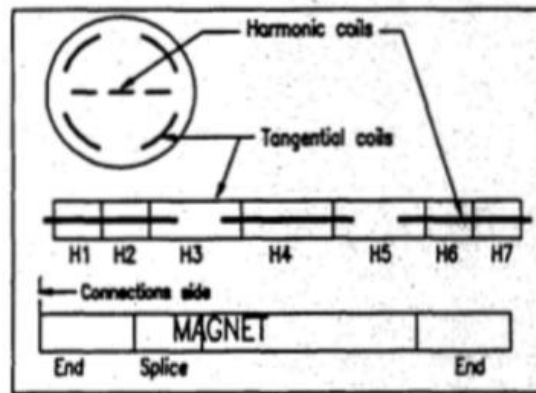
# Magnetic quench antennas

# First quench antennas

A less invasive tool to detect and monitor disturbances and quench development. Relies on a set of pick-up coils positioned inside the bore of the magnet or in a close proximity to magnet windings.

## Beginning of Quench Antenna

- First concept is proposed by Jacek Krzywinski in early 1990's
  - "Quench Observation in LHC Superconducting One Meter Dipole Models by Field Perturbation Measurements," D. Leroy et.al. 1993
  - Adapted for two in one magnet; use other aperture for noise cancel



# Quench antenna

A less invasive tool to detect and monitor disturbances and quench development. Relies on a set of pick-up coils positioned inside the bore of the magnet or in a close proximity to magnet windings.

- Detect Magnetic Field Perturbation caused by current redistribution in quench front

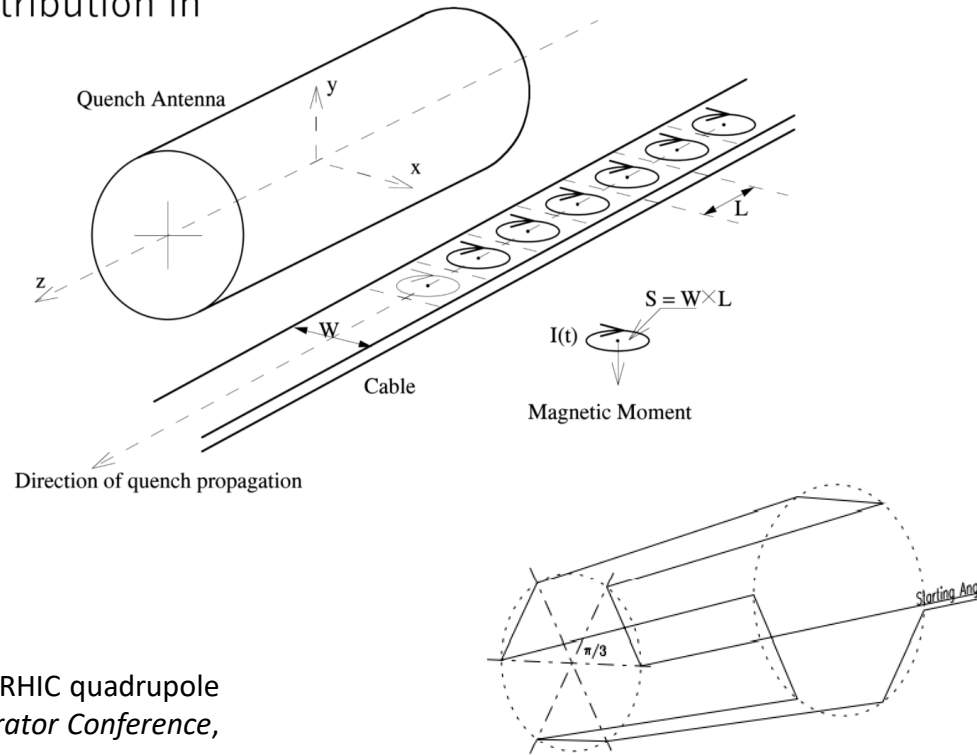
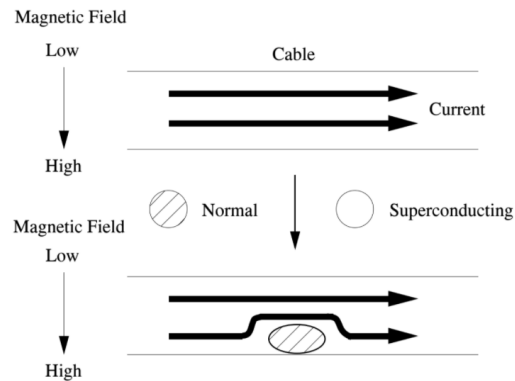


Figure 1b Three dimensional view of a single turn sextupole coil.

T. Ogitsu et al., "Quench antennas for RHIC quadrupole magnets," *Proceedings Particle Accelerator Conference*, Dallas, TX, USA, 1995, pp. 1390-1392

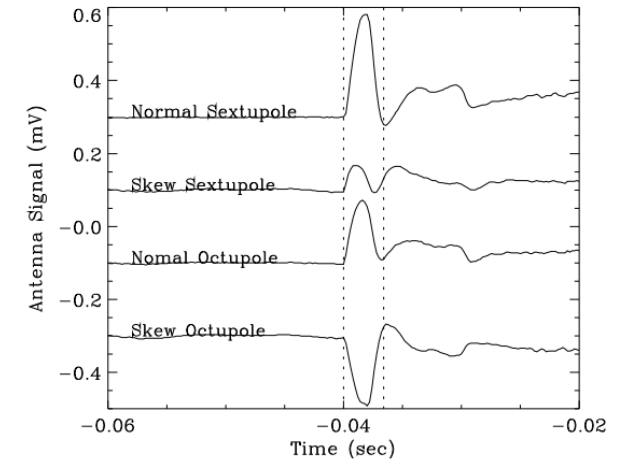


Figure 3a Signals of the coils in C-1. The signals are offset.

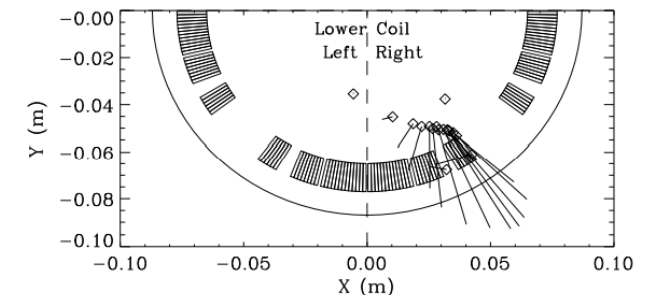
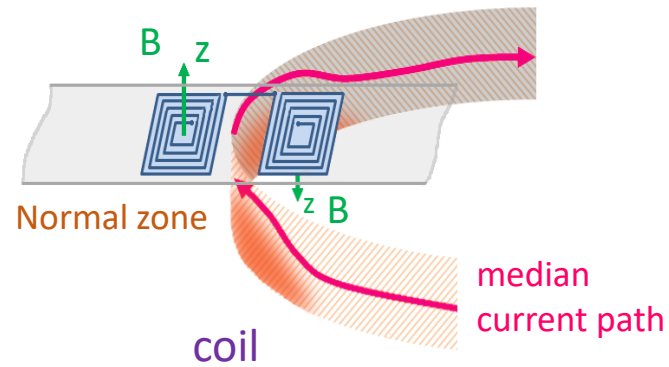
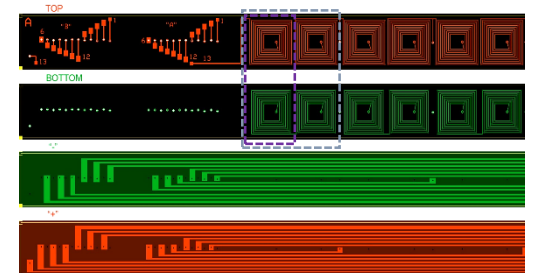
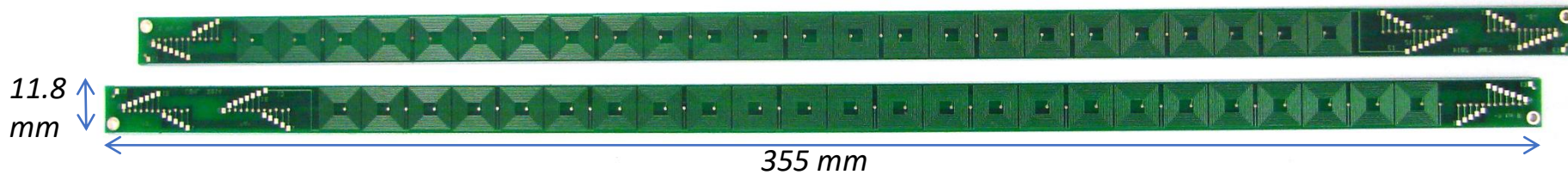


Figure 3b Azimuthal quench localization, as viewed from the lead end.

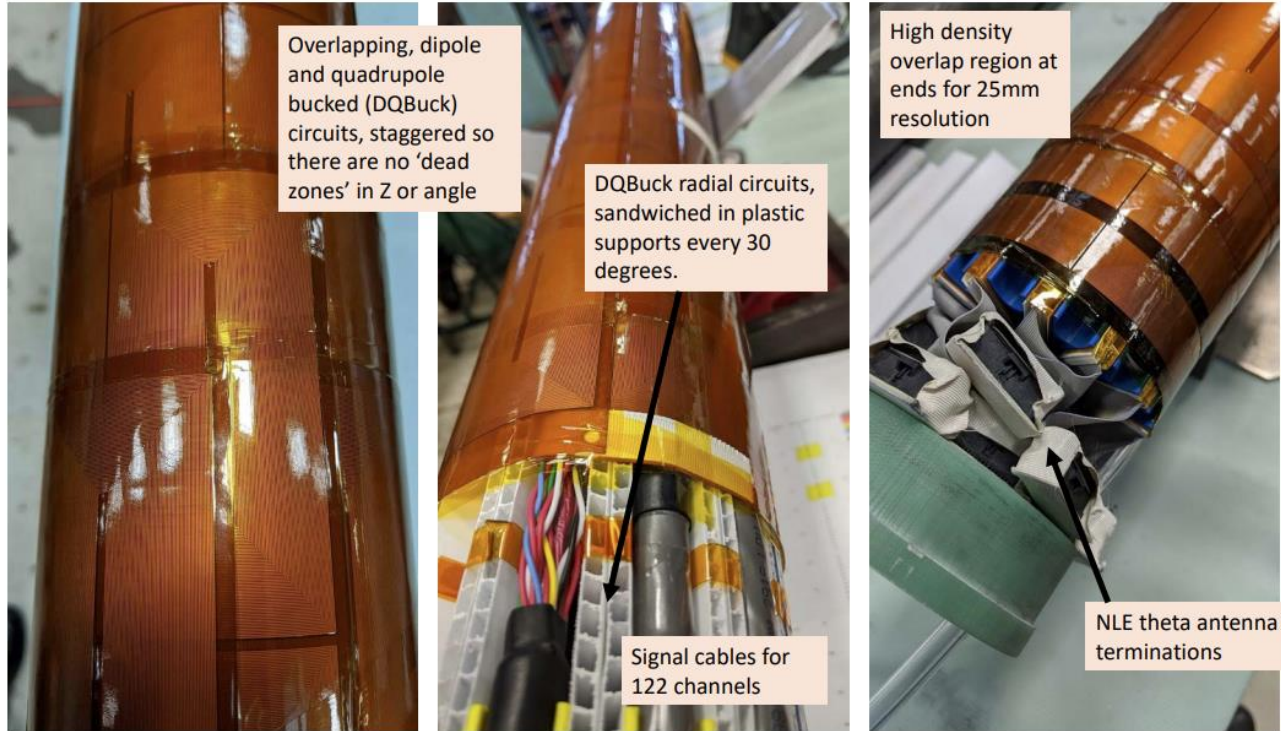
# Linear array PCB antenna (CCT)



A linear array of 24 printed square coils (each is 2 layers, ~20 turn total, ~1 cm side). Coils are dipole-bucked thus forming 12 independent sensors per array. Two arrays can be further “stacked” linearly with a flat ribbon jumper, to have all 24 sensors interfaces from one end of the assembly.



# Flexible PCB-based quench antennas



*J. DiMarco, S. Stoynev, FNAL*



*R. Teyber, D. Arbelaez, LBNL*

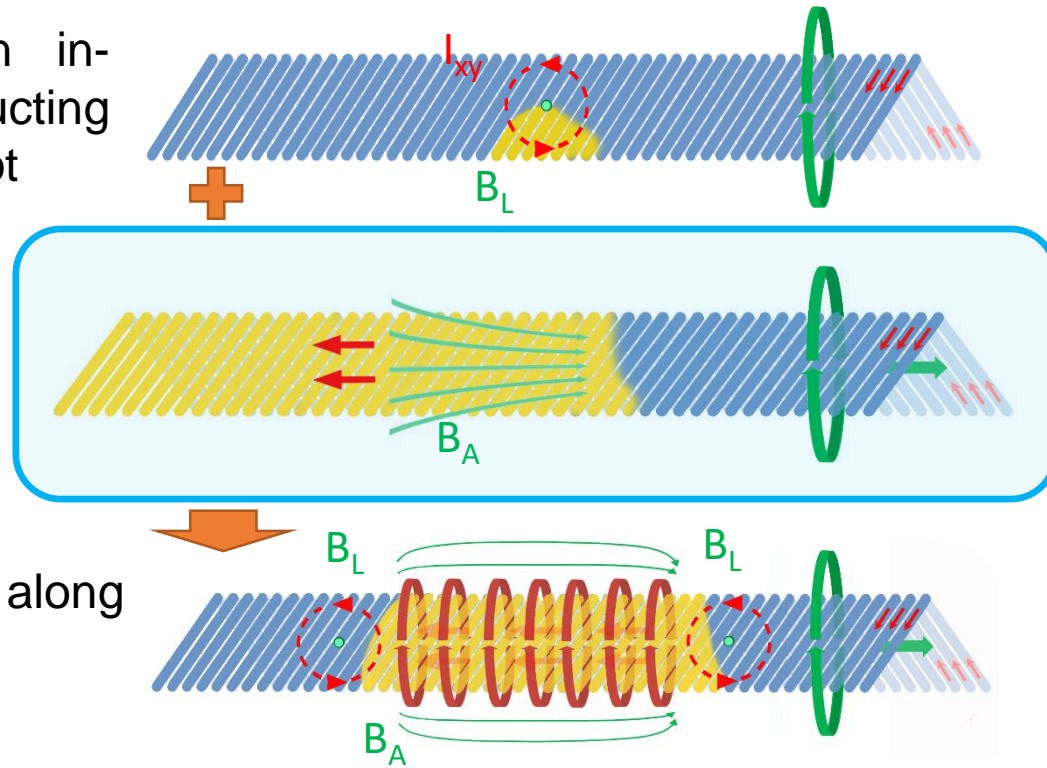
# Axial field “quench antenna”: the principle of operation

Field variation due to a developing quench:

1. Current re-distribution in-plane of the superconducting cable: avoiding the hot spot

2. Breakdown of a solenoidal current path in the cable

3. Normal zone expands along the cable



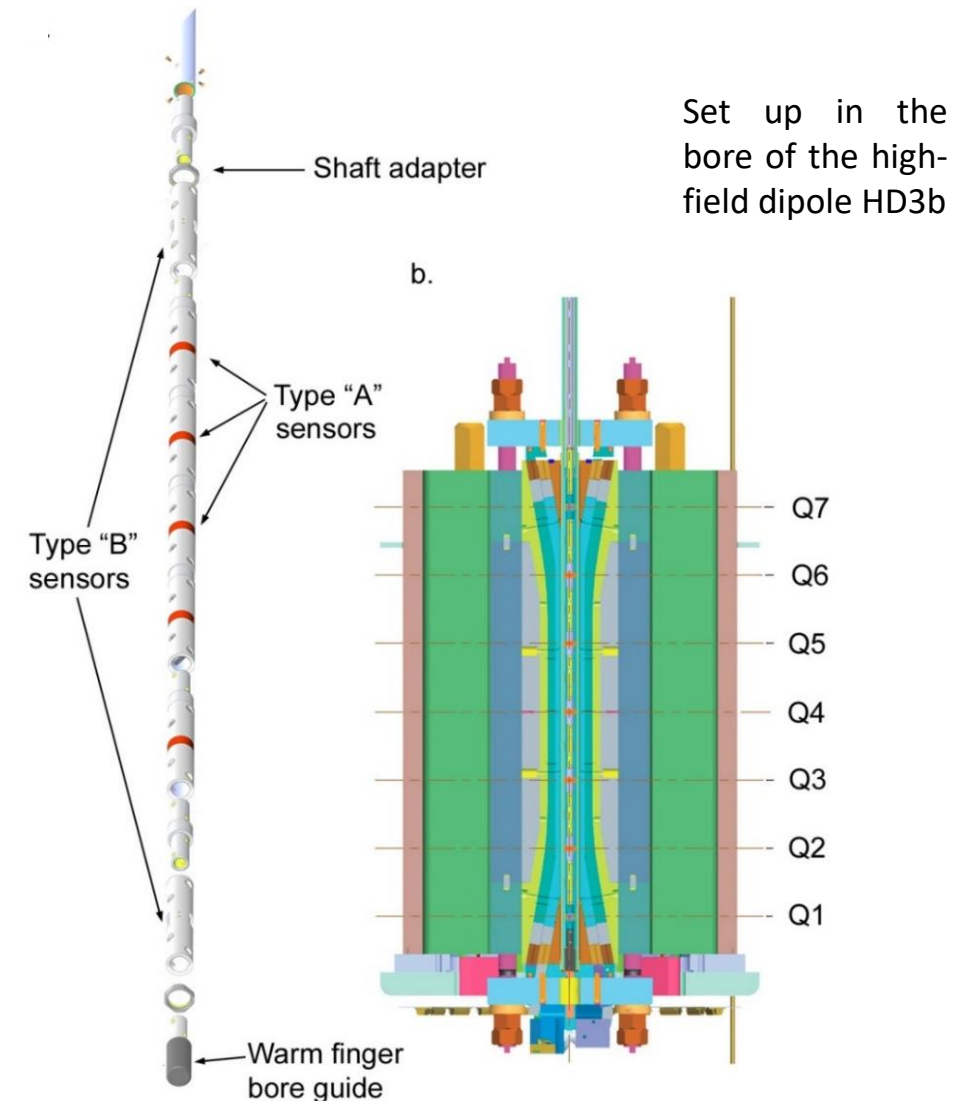
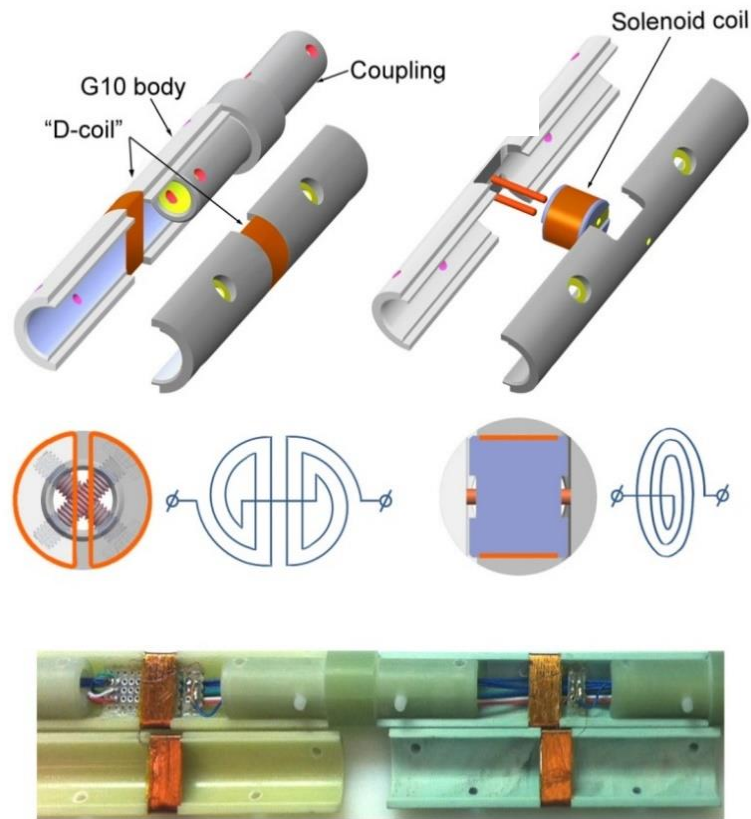
Relying on the axial field component for quench localization has some advantages:

- Better S/N ratio (as accelerator magnets normally **do not have** axial field inside bore)
- Less shielding by the walls of the bore tube (and/or the anti-cryostat), especially at high frequencies

“Magnetic Detection of Quenches in High-Field Accelerator Magnets”, M. Marchevsky, J. DiMarco, H. Felice, A. Hafalia, J. Joseph, J. Lizarazo, X. Wang, G. Sabbi, *IEEE Trans. Appl. Supercond.* 23, 9001005 (2013), DOI: 10.1109/TASC.2012.2236379

# Axial field quench antenna II (dipole adapted)

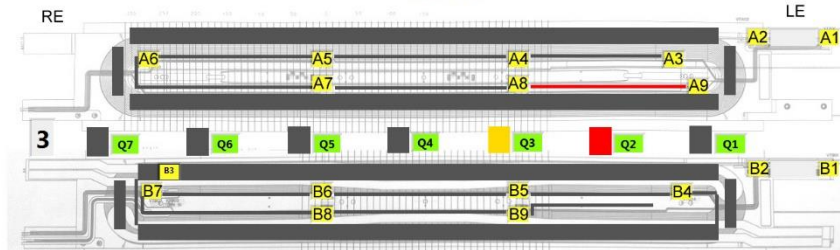
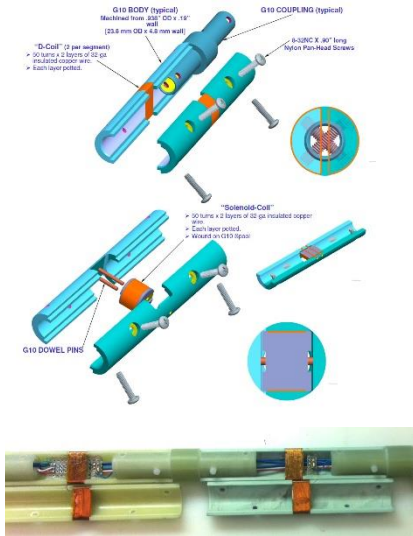
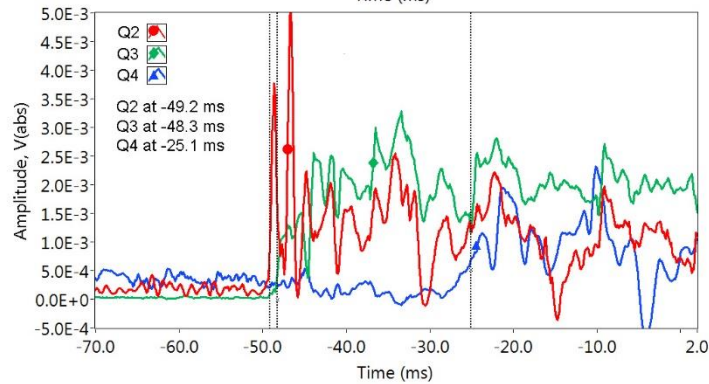
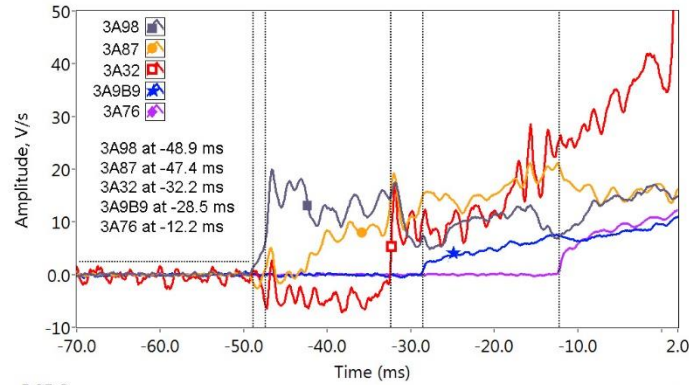
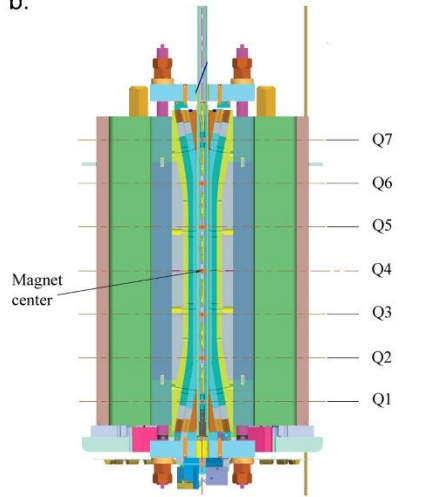
Senses off-axis gradient of the axial field



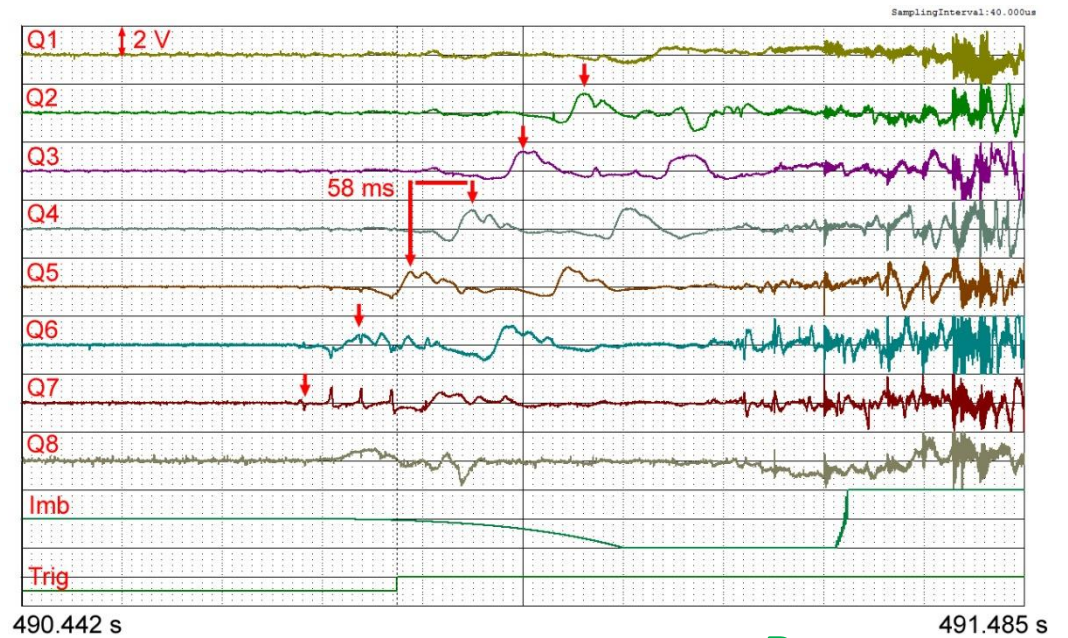
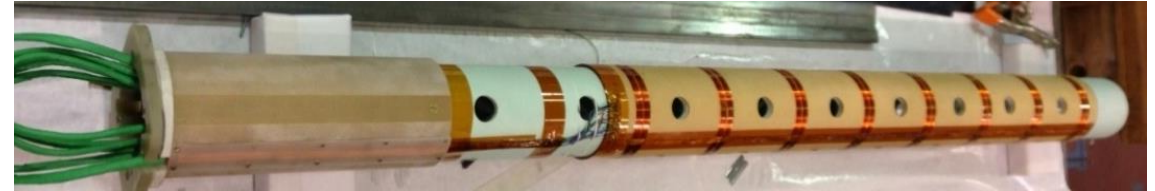
"Axial-Field Magnetic Quench Antenna for the Superconducting Accelerator Magnets", M. Marchevsky, A. R. Hafalia, D. Cheng, S. Prestemon, G. Sabbi, H. Bajas, G. Chlachidze, *IEEE Trans. Appl. Supercond.* 25, 9500605 (2015), DOI: 10.1109/TASC.2014.2374536



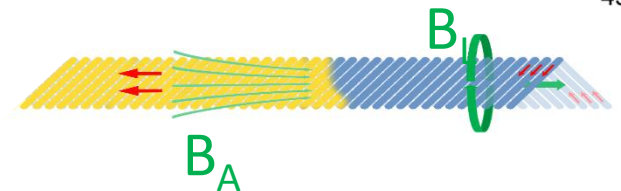
b.



Senses axial gradient of the axial field

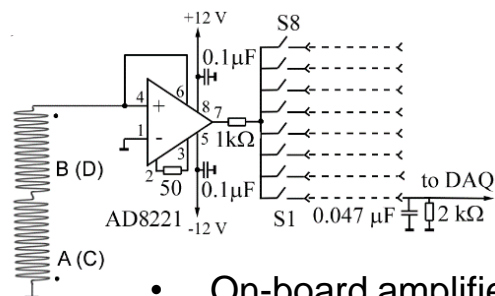
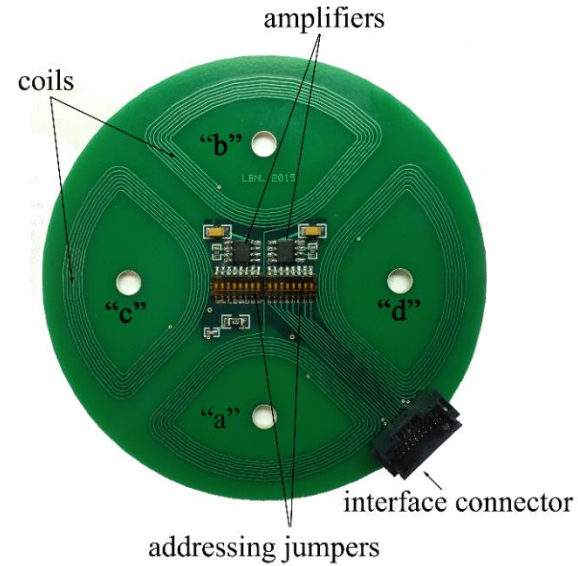


Breakdown of a solenoidal current path in the cable



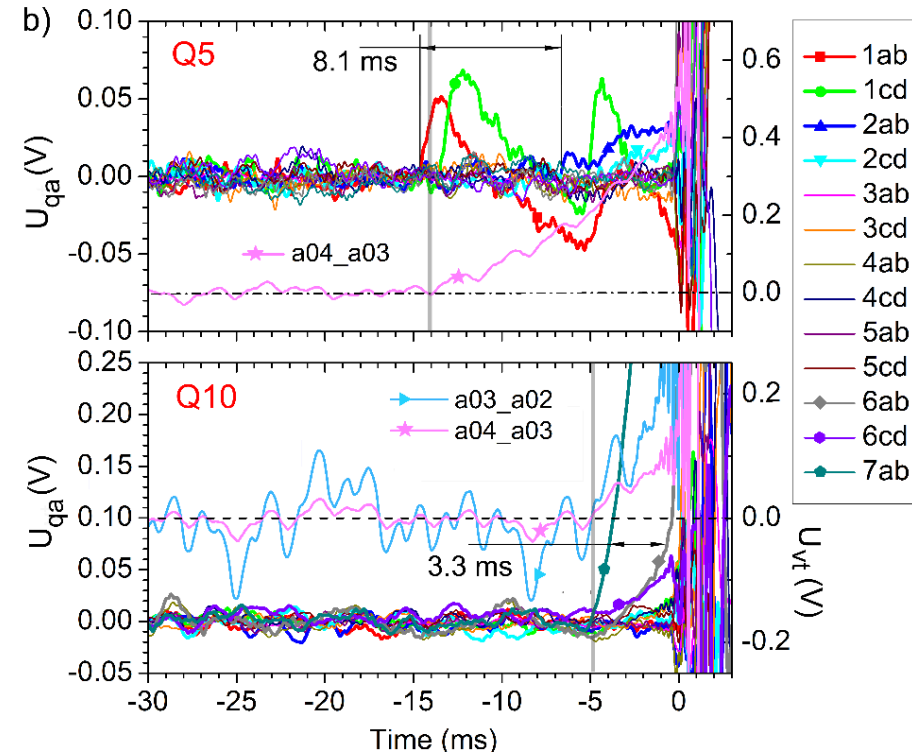
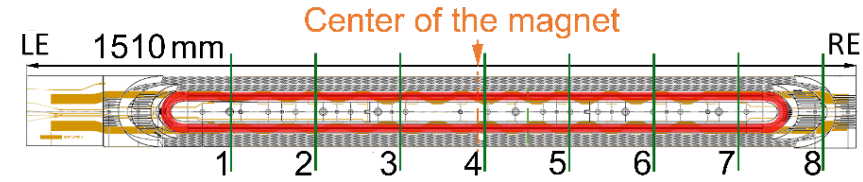
# Round PCB antenna (QXF quadrupole adapted)

Senses off-axis gradient of the axial field



- Modular design

- On-board amplifier

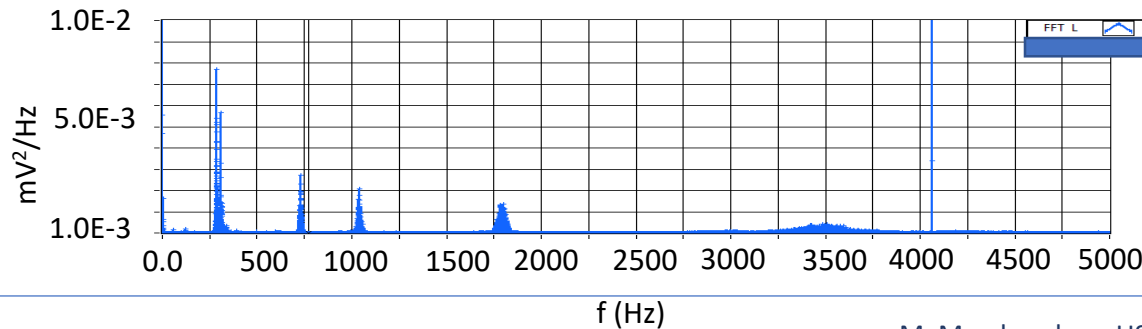
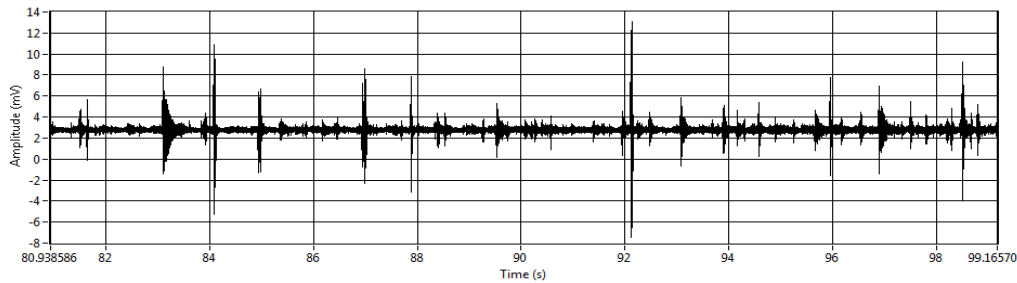
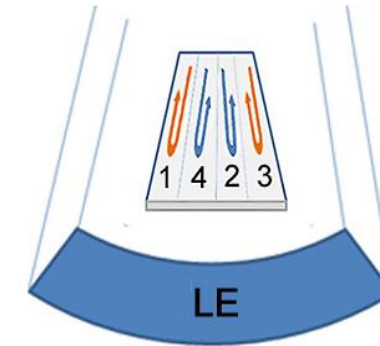
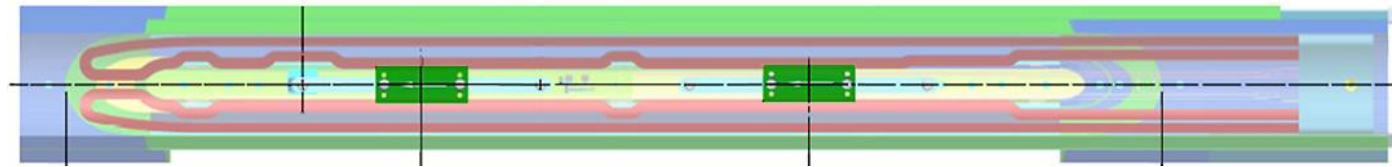
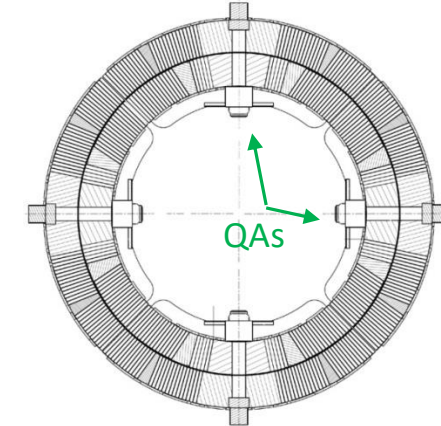
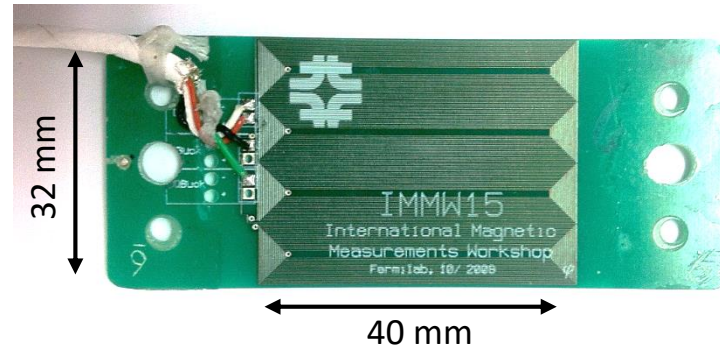


Quench localization in MQXF-S quadrupole

“Magnetic Quench Antenna for MQXF quadrupoles”, M. Marchevsky, G. Sabbi, S. Prestemon, T. Strauss, S. Stoynev and G. Chlachidze, IEEE Trans. Appl. Supercond. 27, v. 4, 9000505 (2017), DOI: 10.1109/TASC.2016.2642983

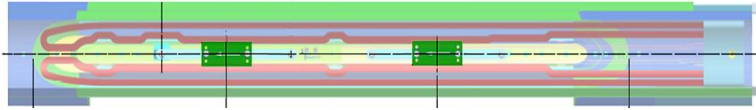
# PC board quench antennas as mechanical activity sensors

Magnetic measurement boards developed by J. DiMarco at FNAL were adapted as “inductive “pickup” sensors in HQ01d quadrupole test



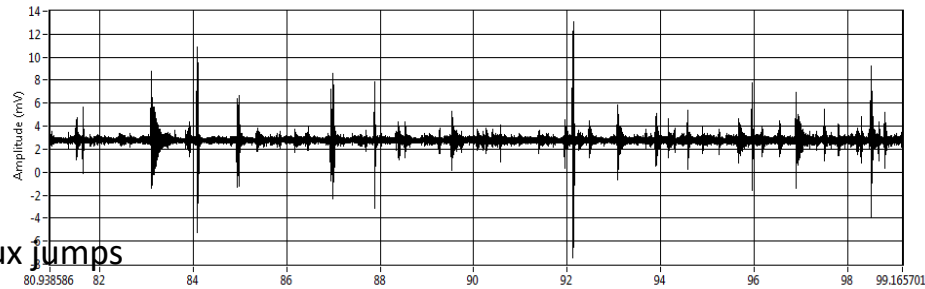
Direct sensing of vibrational coil modes and (possibly) conductor motion!

# Quench antenna as a flux jump sensor

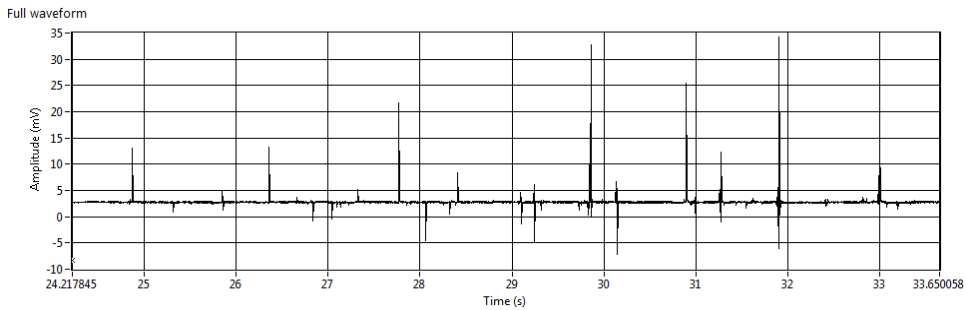


- Dynamics of flux-jumps instabilities can be revealed and their propagation velocities measured.

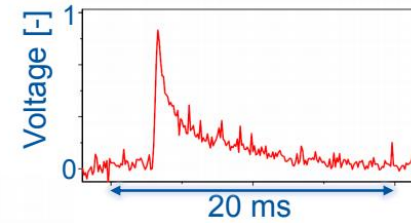
## Mechanical



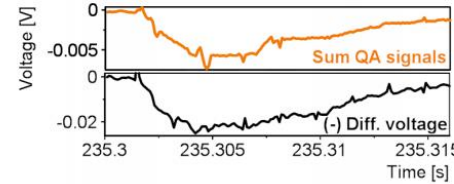
## Flux jumps



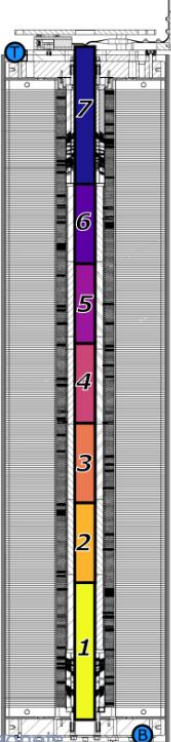
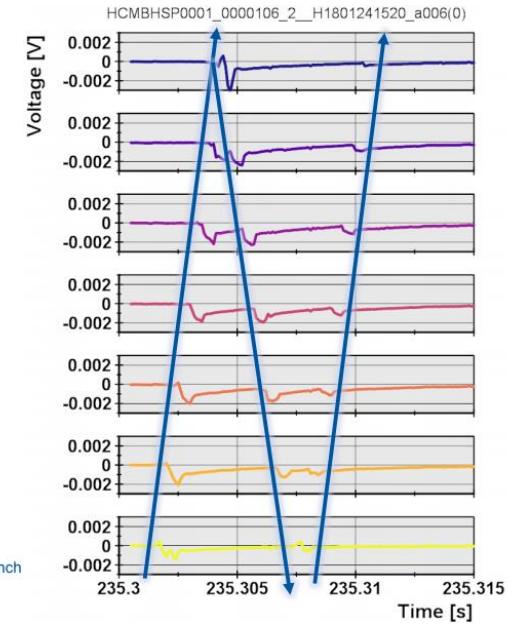
## Example of flux jump in QA:



The sum of QA signals is similar to what is picked up by the differential voltage:



Flux jumps can be seen to propagate with velocities between 500 – 1000 m/s:



- An easy way to distinguish between flux jumps and mechanical instabilities

Flux jump propagation already shown before with similar velocity in Maxim Marchevsky et al., "Axial-Field Magnetic Quench Antenna for the Superconducting Accelerator Magnets" IEEE Trans. Appl. Supercond., Vol. 25, No. 3, 2015, 9500605



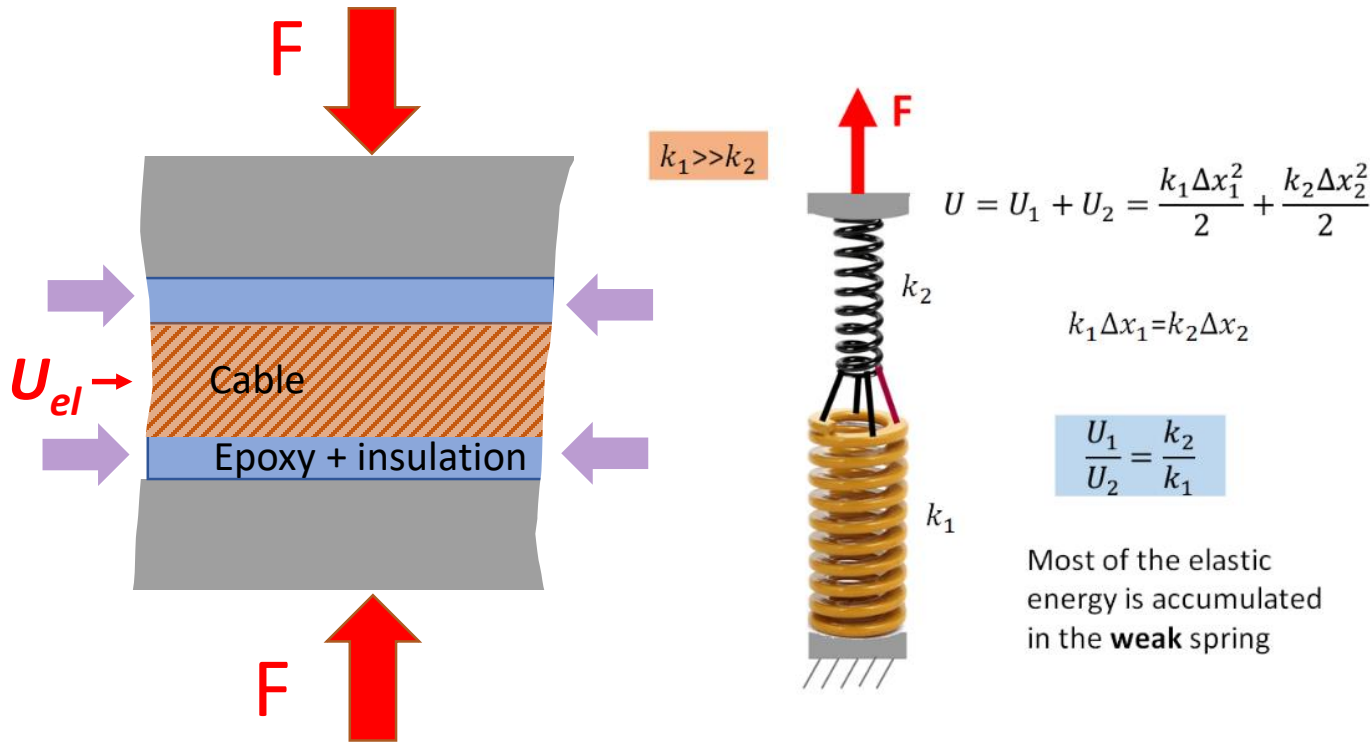
IDSM01 4/24/2019

Michal Duda - Measurement of Electrical and Mechanical Transients in Nb3Sn Magnets



# Detecting mechanical transients and localizing quenches using acoustic emission

# Accumulation and release of the elastic energy



...it seems that the most natural way is to assume that the releasing energy of each event  $E_r$  is proportional to the density of elastic energy, the  $\sigma^2$ , where  $\sigma$  - mechanical stress at the pulse. It is evident that for magnets this is equivalent to  $E_r \sim J^4$  or  $E_r \sim B^4$  where  $J$  - is the

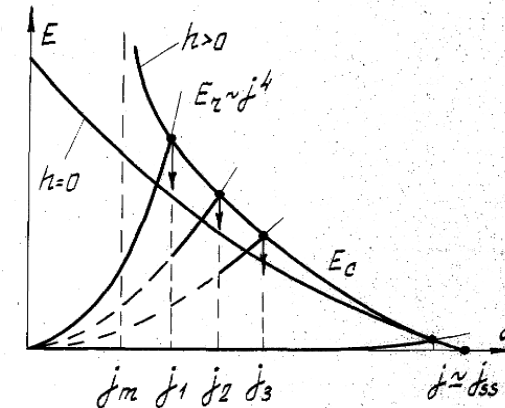
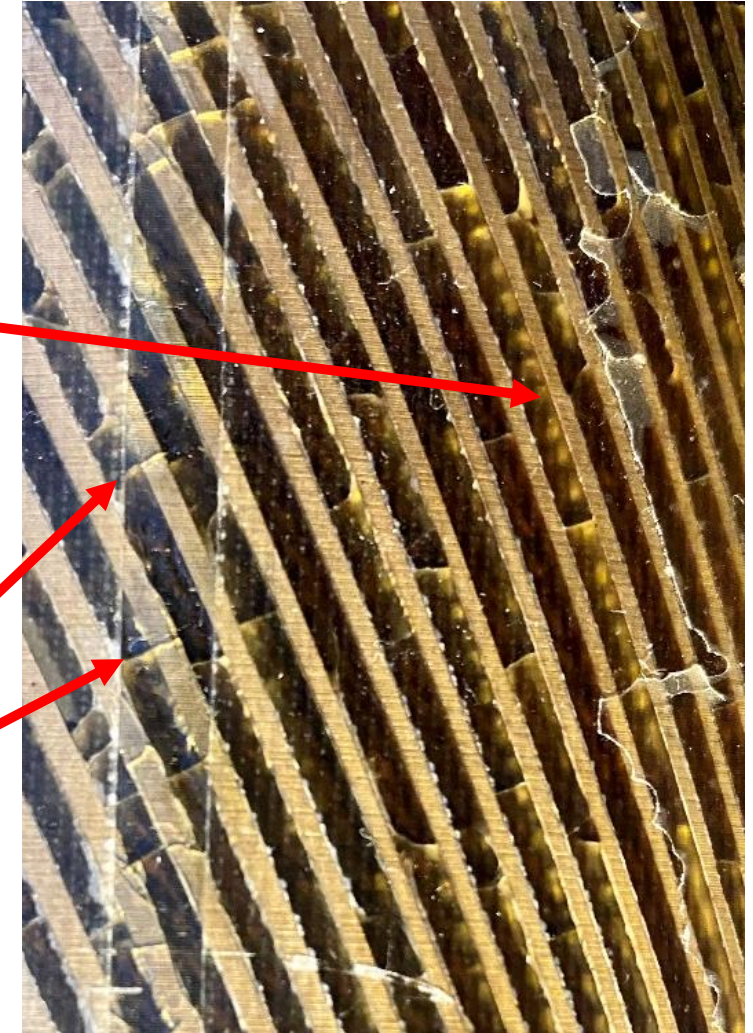
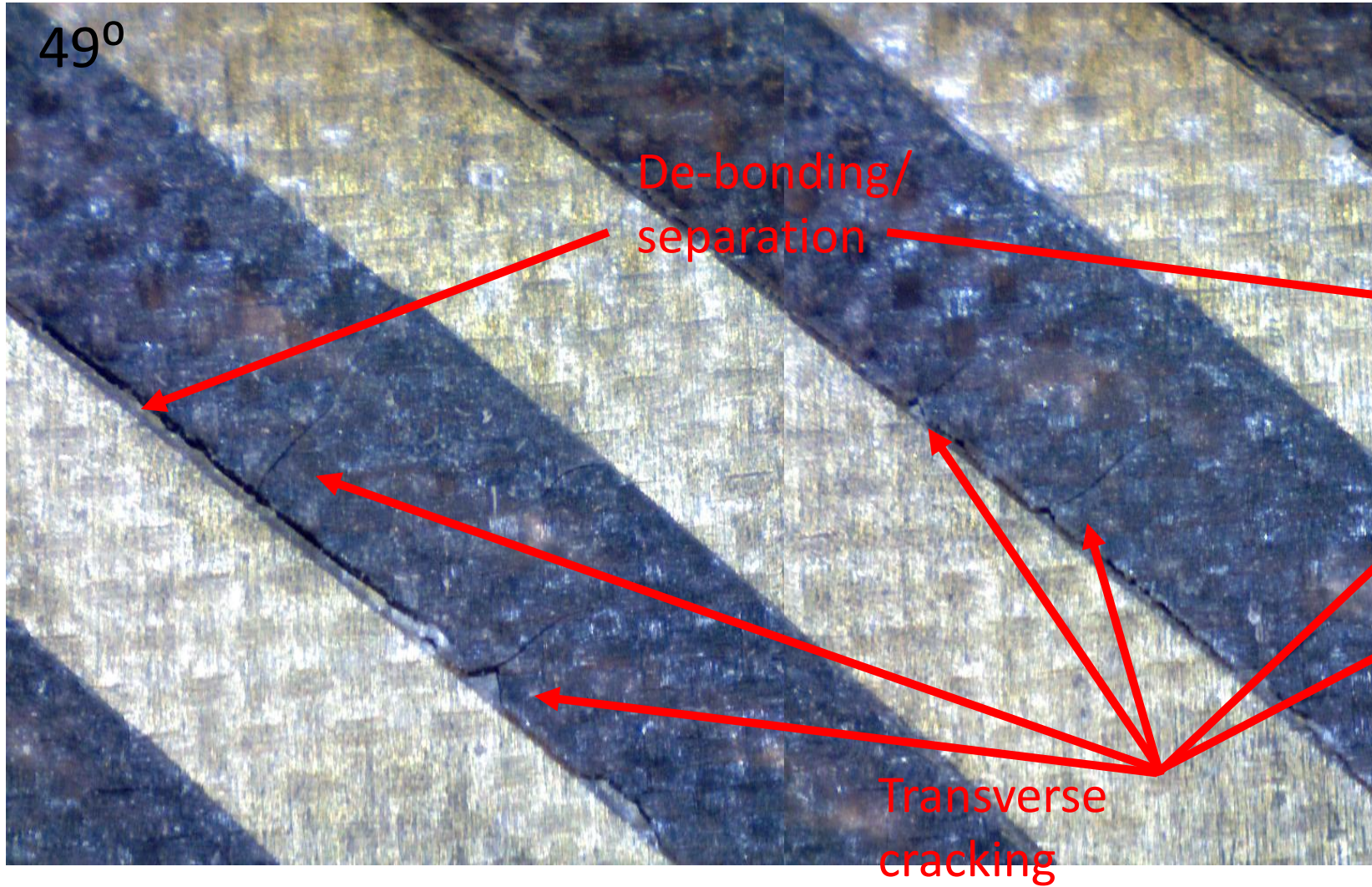


Fig 1 Critical ( $E_c$ ) and releasing ( $E_r$ ) energies vs current density  $j$  of the winding. The intersection points correspond to subsequent quenches.

IEEE TRANSACTIONS ON APPLIED SUPERCONDUCTIVITY, VOL. 3, NO. 1, MARCH 1993 297  
 EXPLANATION OF MAIN FEATURES OF SUPERCONDUCTING WINDING TRAINING BY BALANCE OF ACTING AND PERMISSIBLE DISTURBANCES  
 V.E.Keilin



*D. Arbelaez, LBNL*

CCT4 dipole, IL

# Causes of acoustic emission in magnets

## Singular events

### Mechanical

- **Cracking / fracture of epoxy, de-laminations**
- Sudden mechanical motion of conductor or structural part

### Electromagnetic -> Mechanical

- Flux jump, as current re-distribution in the cable leads to the local variation of the electromagnetic force

## Continuous perturbations

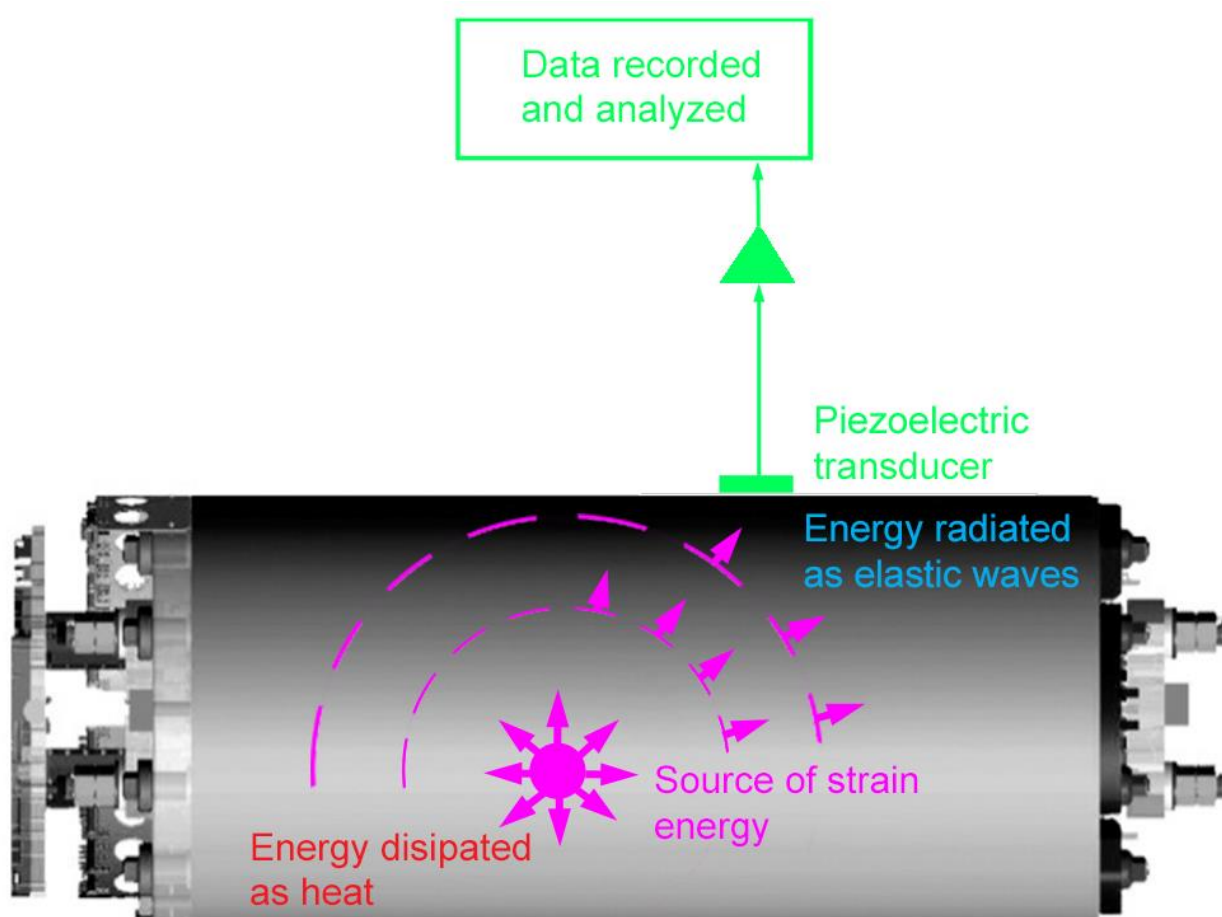
- Vibrations of coils, shell and support structures)
- Background noise (helium boiling, pumps, etc.)

- **Quench development** leads to a local thermal expansion and change in the local stress at sub-millisecond time scale, which *may* lead to acoustic emission. However, magnets that are conductor-limited are near-quiet acoustically at quench.

- “Acoustic emission from NbTi superconductors during flux jump”, G. Pasztor and C. Schmidt, Cryogenics 19, 608 (1979).
- “Sources of acoustic emission in superconducting magnets”, O. Tsukamoto and Y. Iwasa, J. Appl. Phys. 54, 997 (1983).



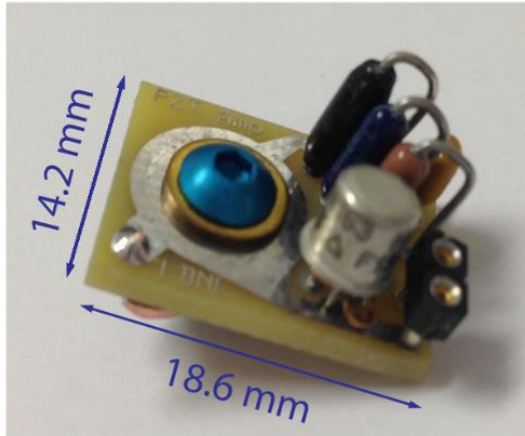
# Advantages of AE diagnostics



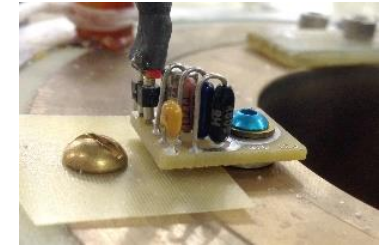
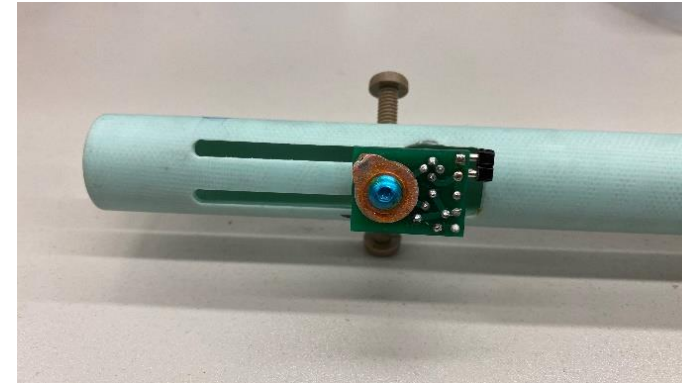
- Sound propagation velocity is several km/s), so that detection time scale is comparable (or faster) to other techniques
- Sound sources can be localized through triangulation
- Sensors can be installed on the outer surfaces – non-intrusive
- Immune to magnetic fields
- Sensors and acquisition hardware are relatively inexpensive, portable and easily adaptable to various magnet configurations

Wave conversion... absorption... acoustic impedance mismatch...

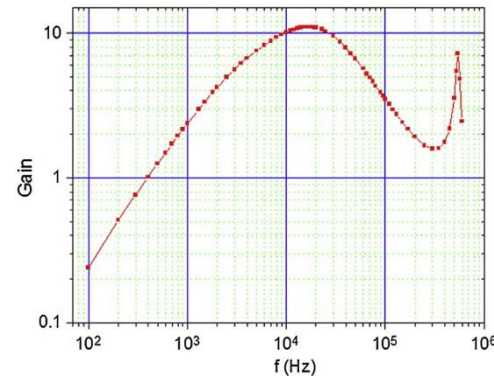
# Amplified piezo-sensors for AE studies



Cryo-amplifier board

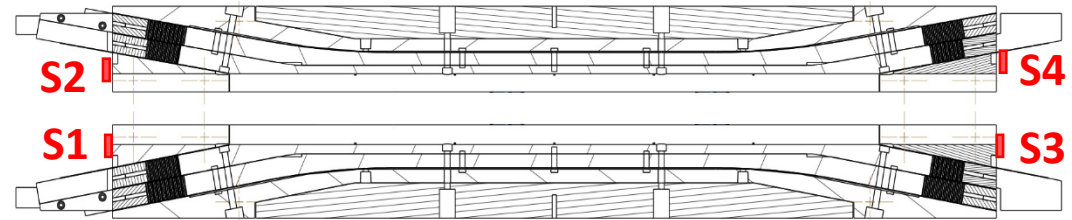


Piezoelectric transducers



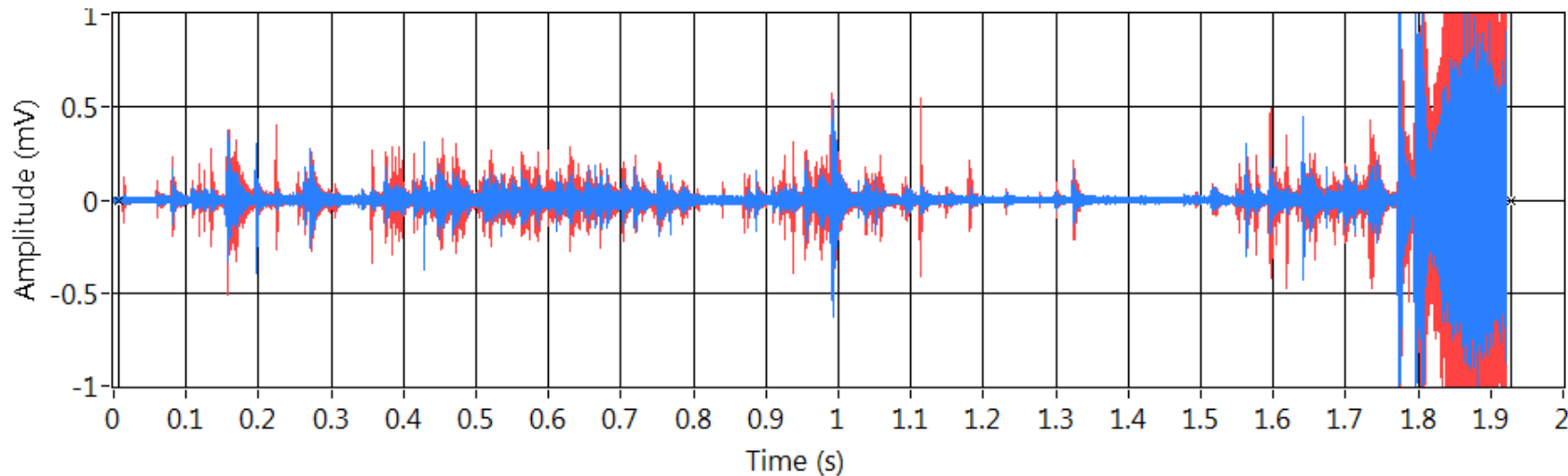
Various AE sensors and mounting hardware (LBNL)

# Nb<sub>3</sub>Sn dipole quench sound example



Sensors are installed at the ends of each 1-m long dipole coil. Multiple acoustic events are recorded during ramping

Quench A76 at 16042 A



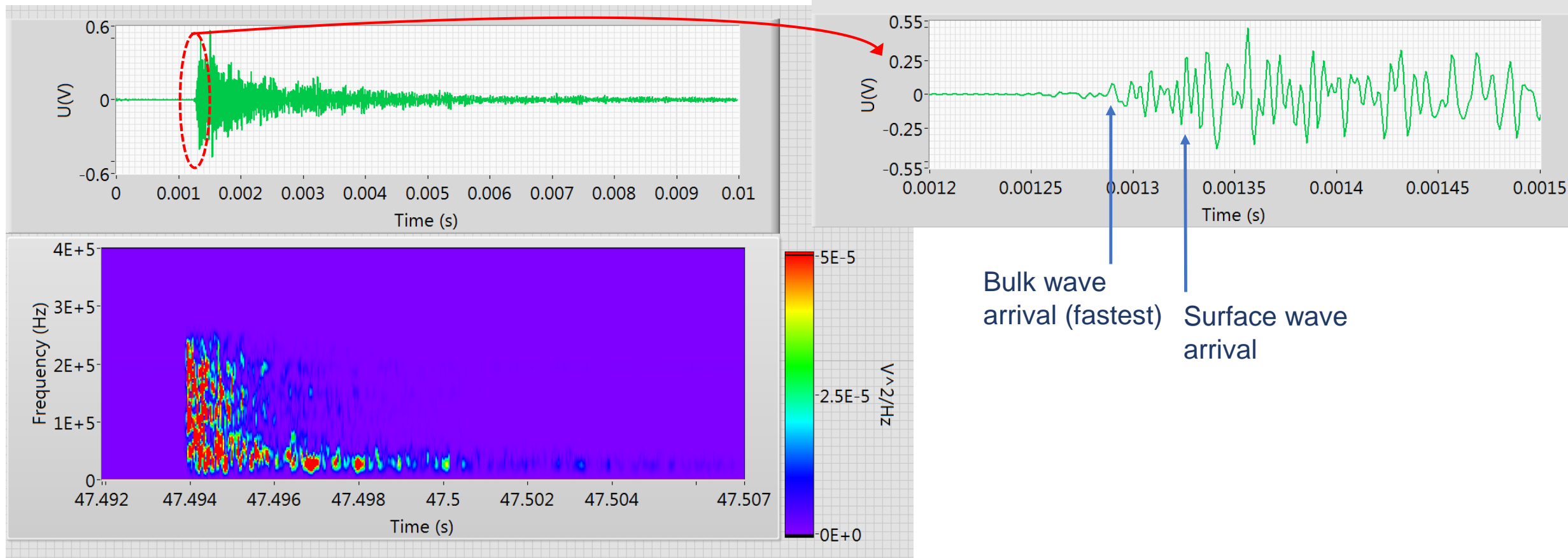
Sensor S1 (blue) -> Left sound channel  
Sensor S4 (red) -> Right sound channel



*Original sound slowed down 10 times*

# Spectrogram of a typical acoustic transient

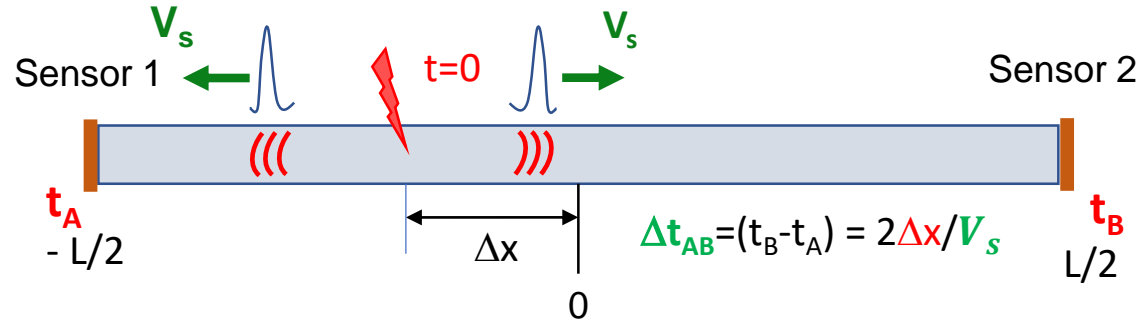
CCT4, ramp to quench #1



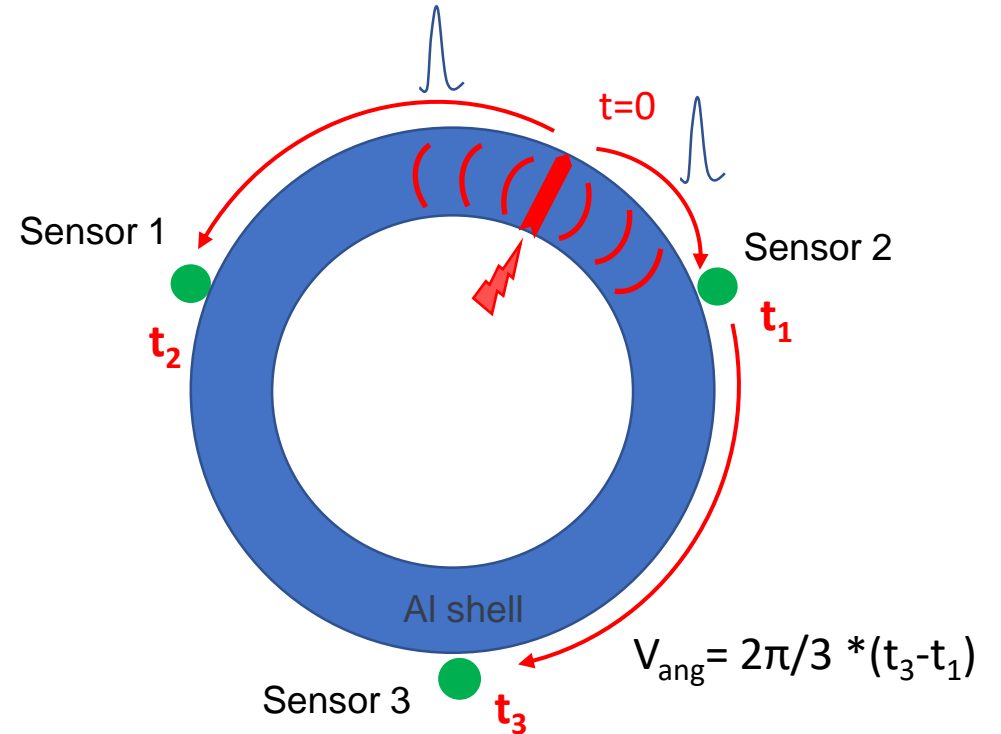
- Frequencies up to ~250 kHz are present
- “Ring down” with a characteristic timescale of 1-5 ms
- Low-frequency “tale”

# Quench localization using AE

## Axial localization



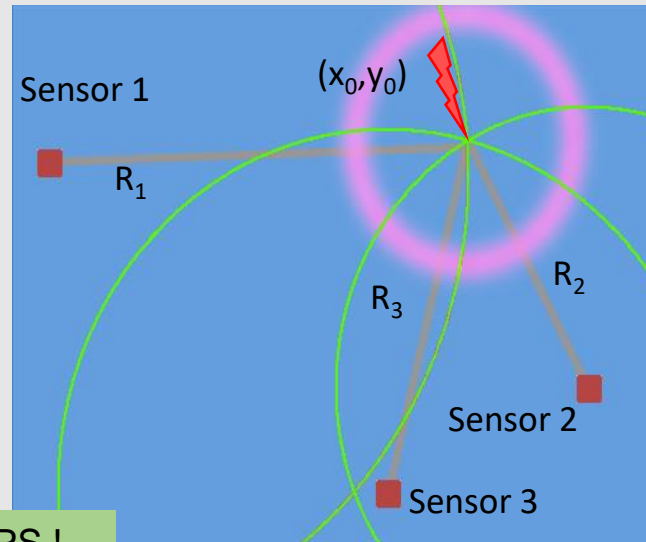
## Angular localization



## 2D (3D) localization

2D

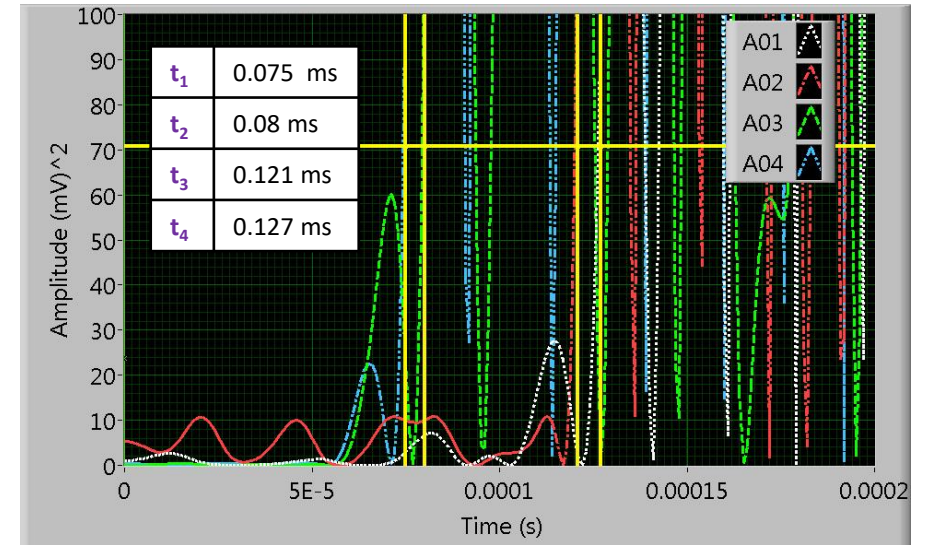
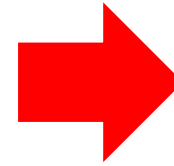
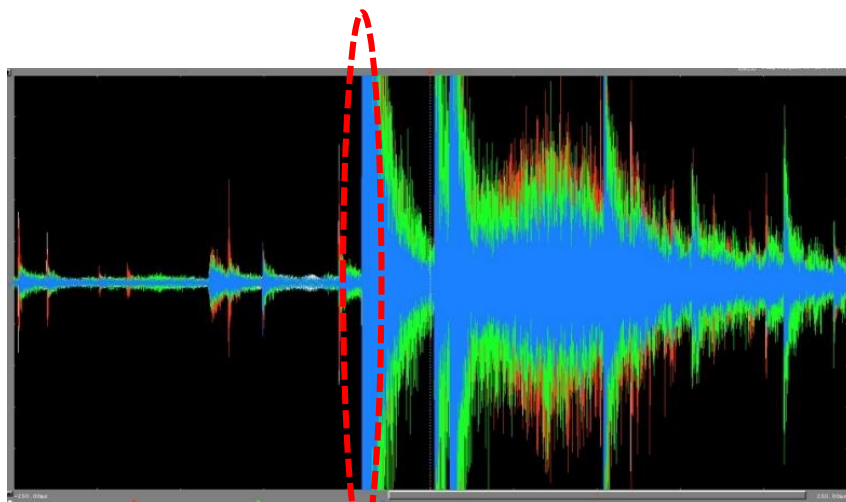
$$\begin{cases}
 (x_0 - x_1)^2 + (y_0 - y_1)^2 = R_1^2 \\
 (x_0 - x_2)^2 + (y_0 - y_2)^2 = R_2^2 \\
 (x_0 - x_3)^2 + (y_0 - y_3)^2 = R_3^2 \\
 |R_1 - R_2| = V_s \Delta t_{12} \\
 |R_1 - R_3| = V_s \Delta t_{13}
 \end{cases}$$



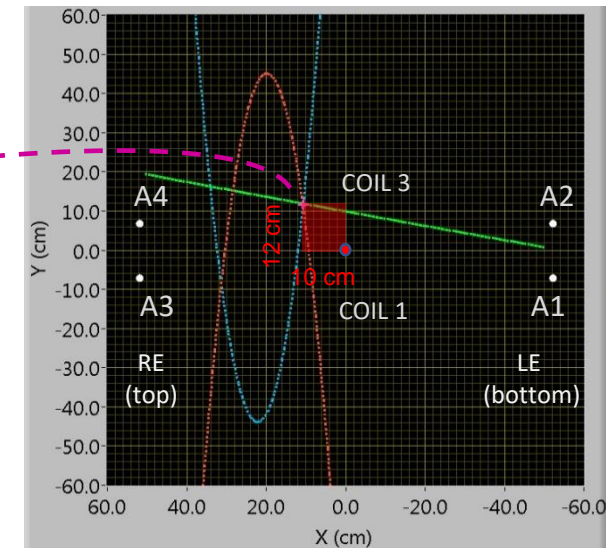
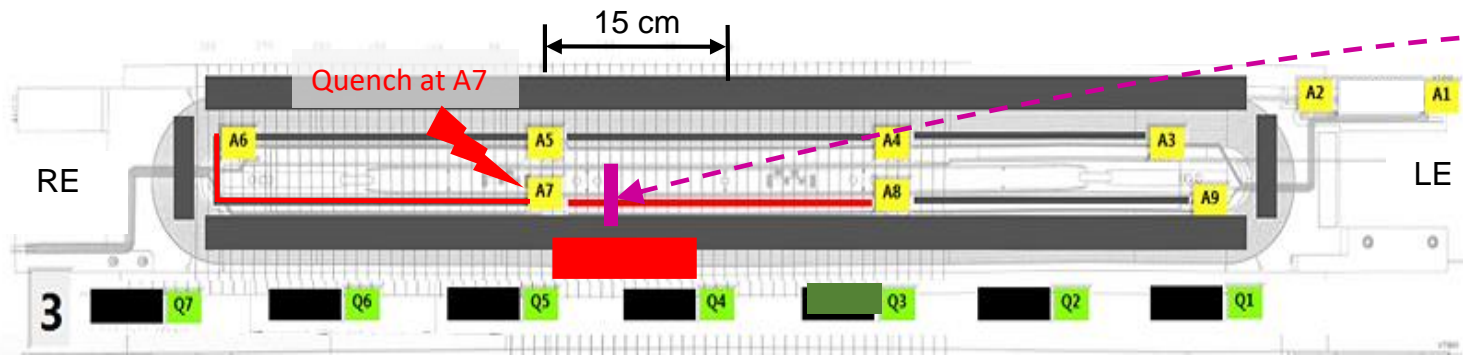
Think GPS!

On a cylindrical surface localization using quasi-2D approach can be sufficiently accurate

# Triangulating a quench in 2D

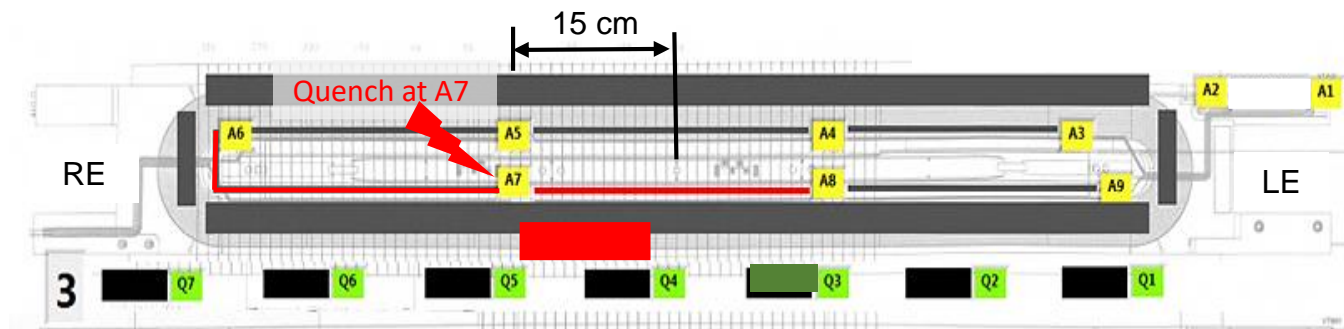
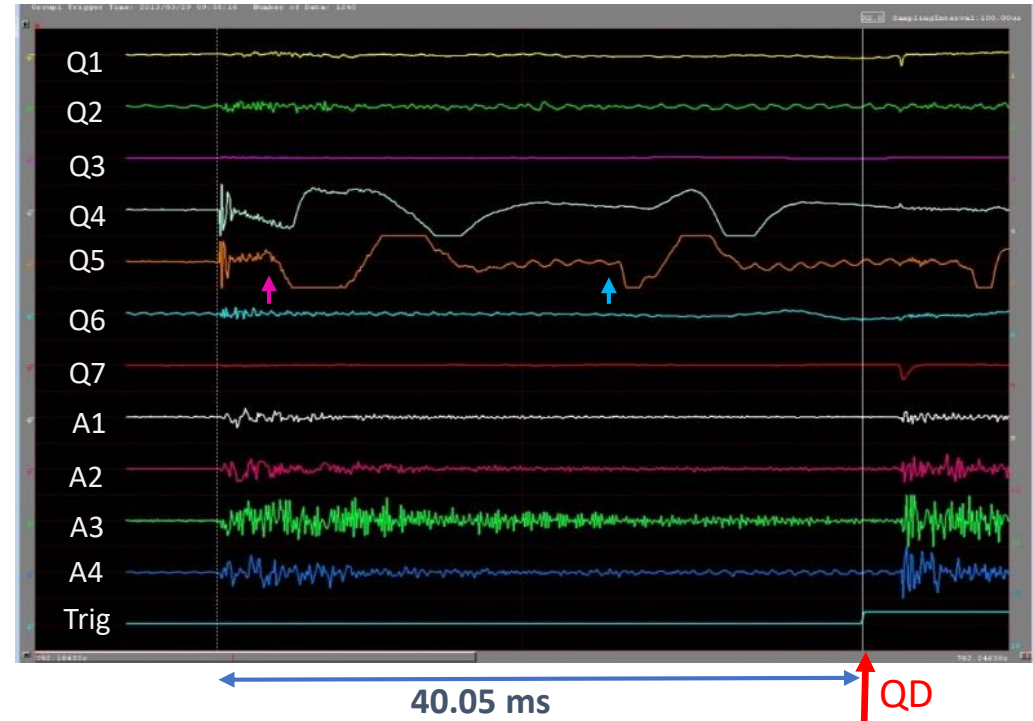
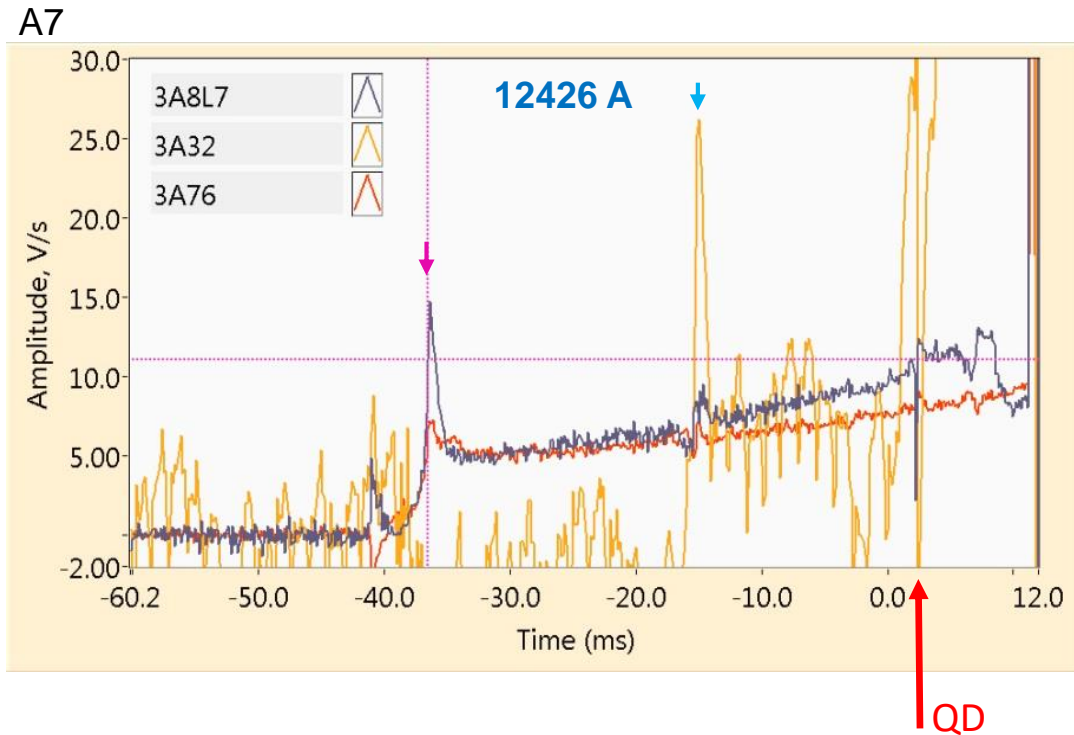
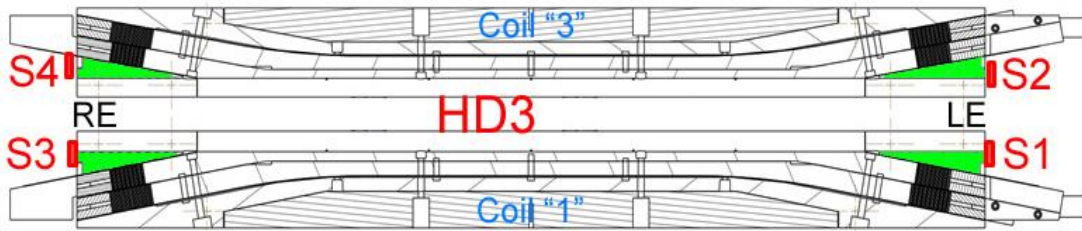


Quench propagation  
40 ms

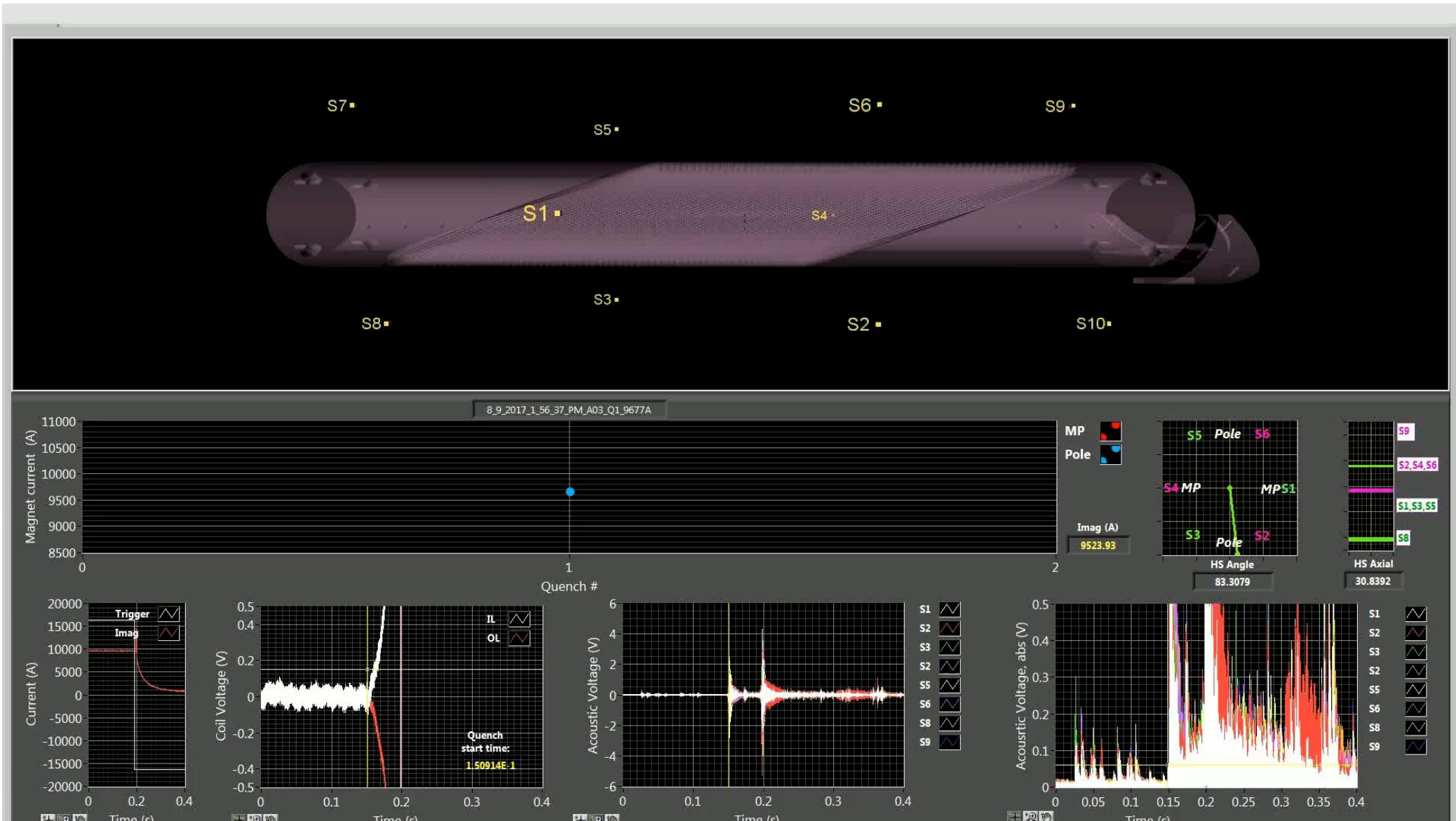


$$v_s = 4.3 \text{ km/s}$$

# Combined diagnostics for quench studies



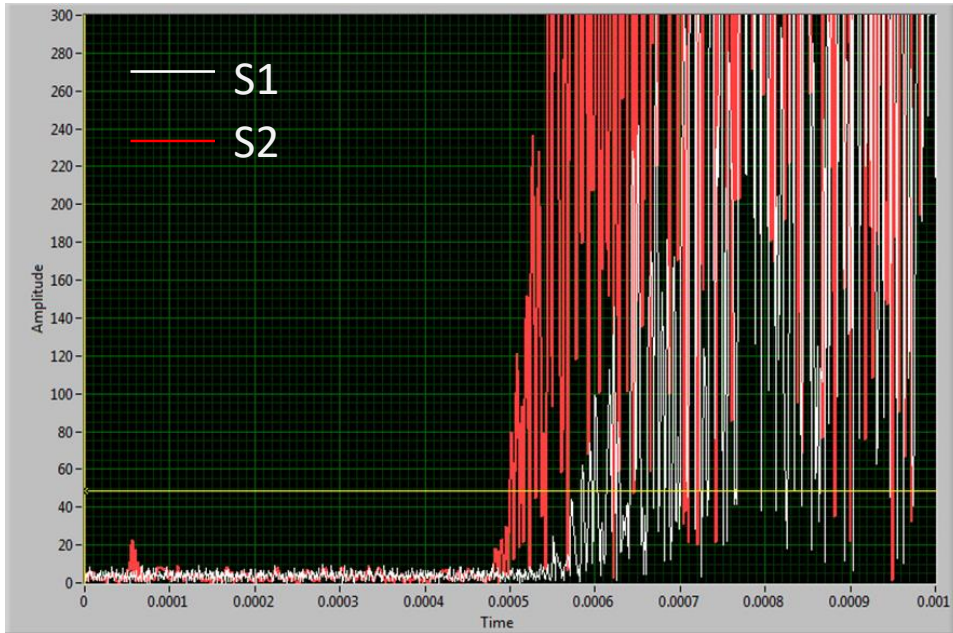
# Example: quench localization in a CCT dipole



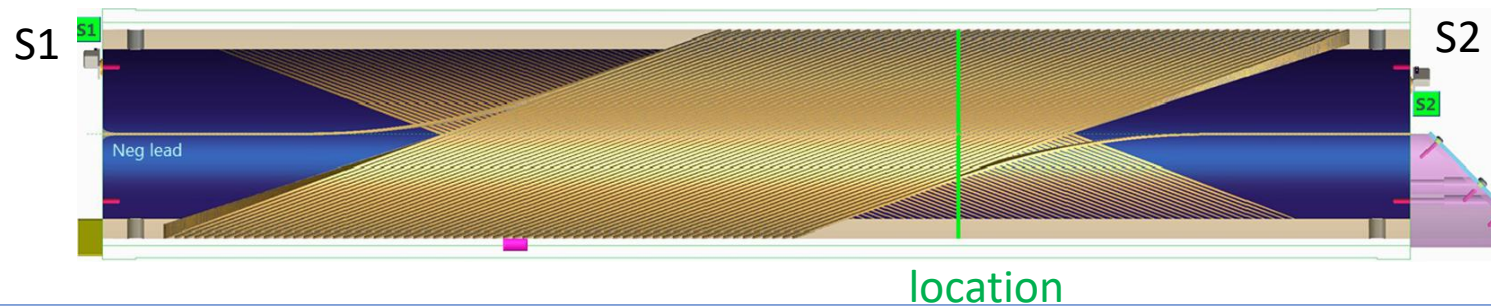
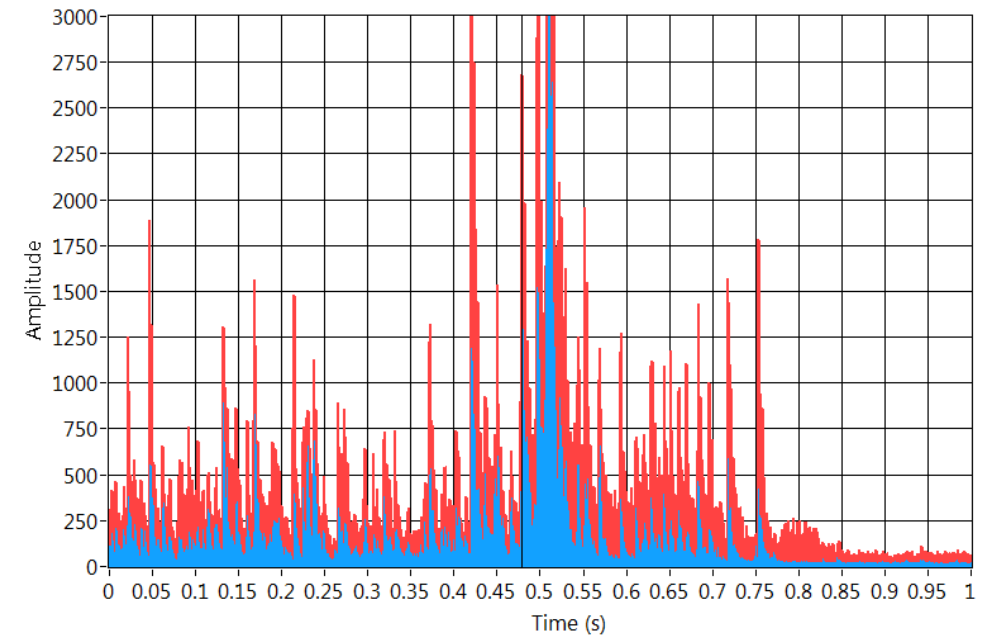


# Localized vs distributed AE sources

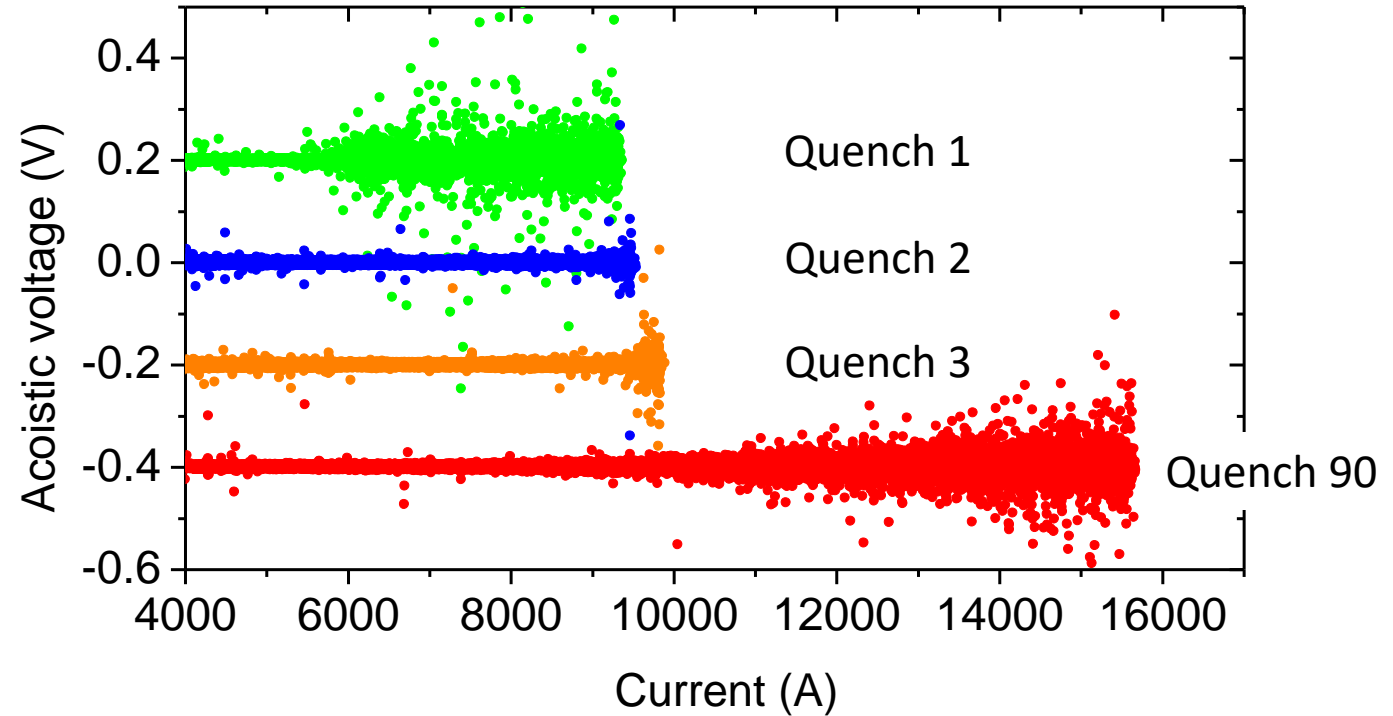
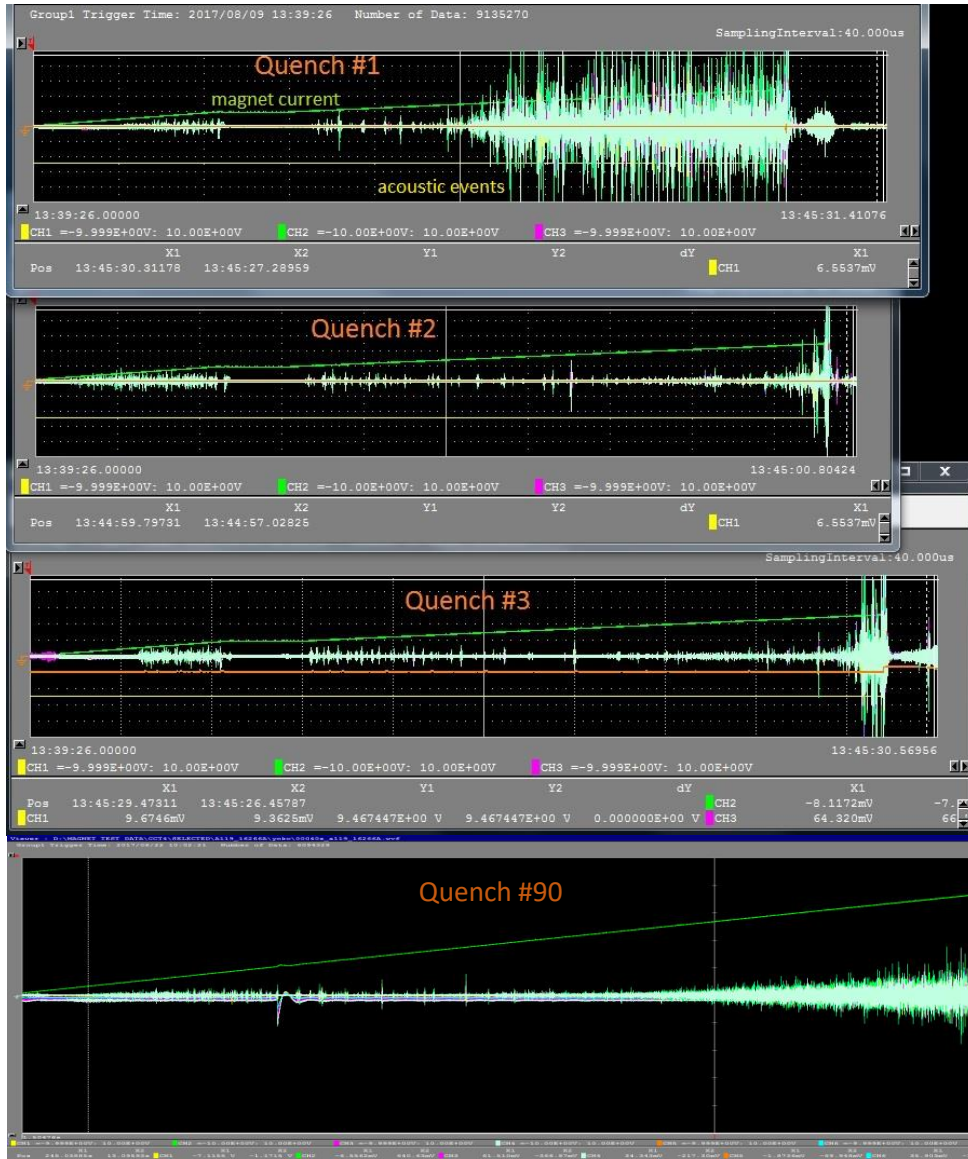
A localized event: information on the azimuthal location



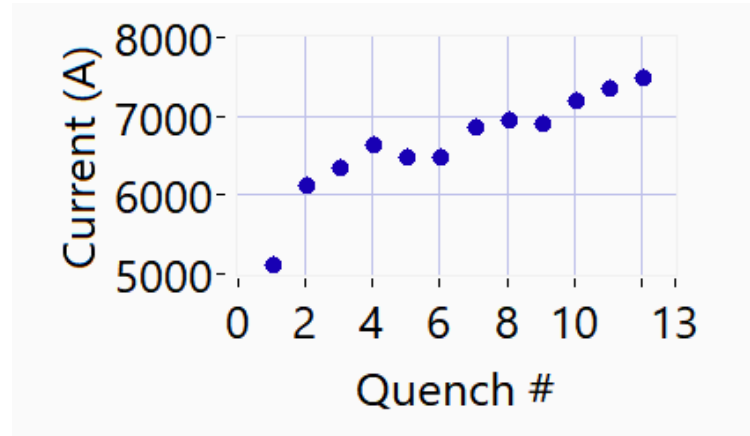
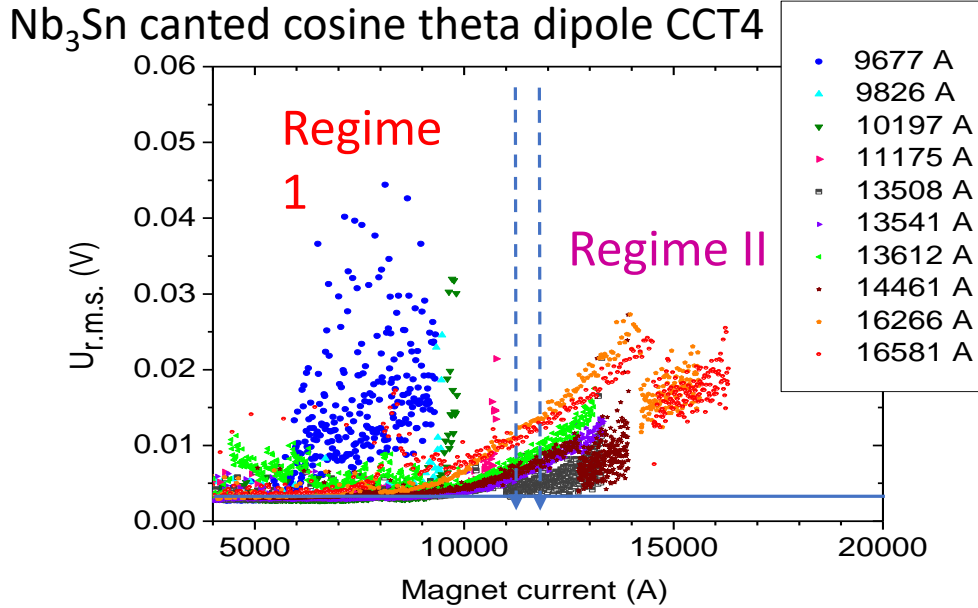
A “distributed” event.... No localization



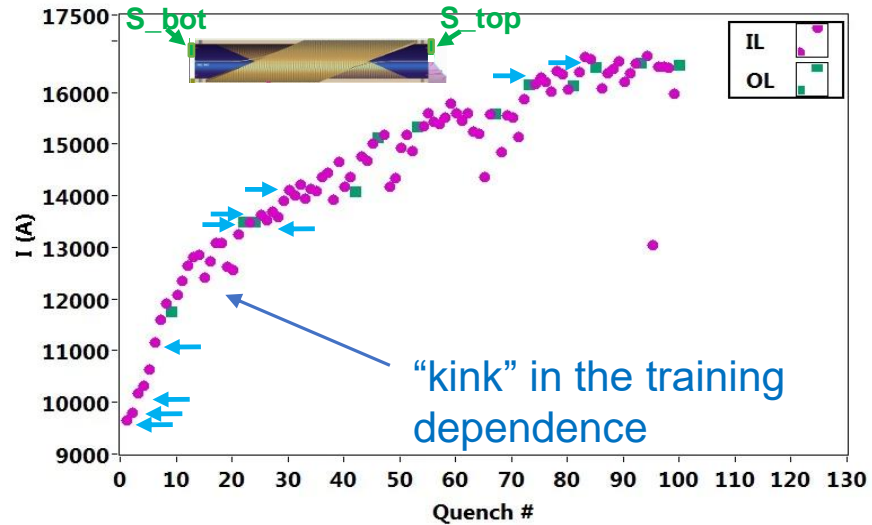
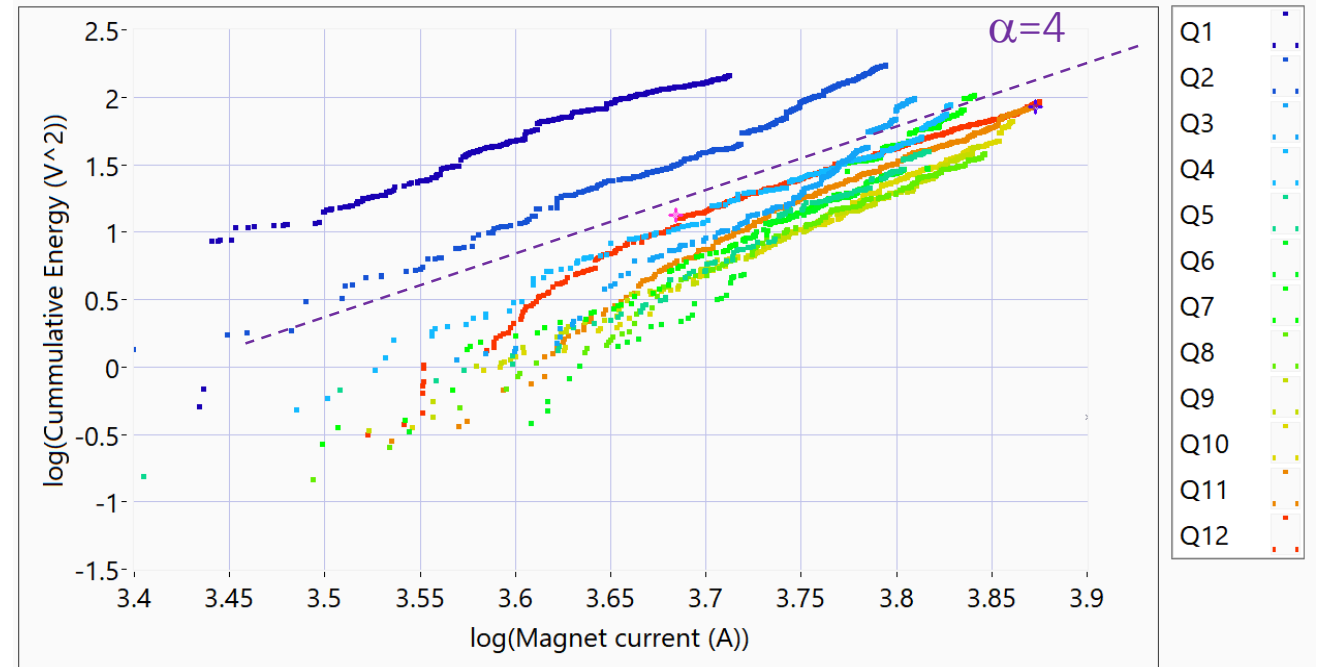
# Mechanical memory of the magnet



- CCT4 magnet shows mechanical memory in the initial quenches (Kaiser effect)
- However, as training progressed, noise grows in amplitude towards the quench, erasing the memory effect.

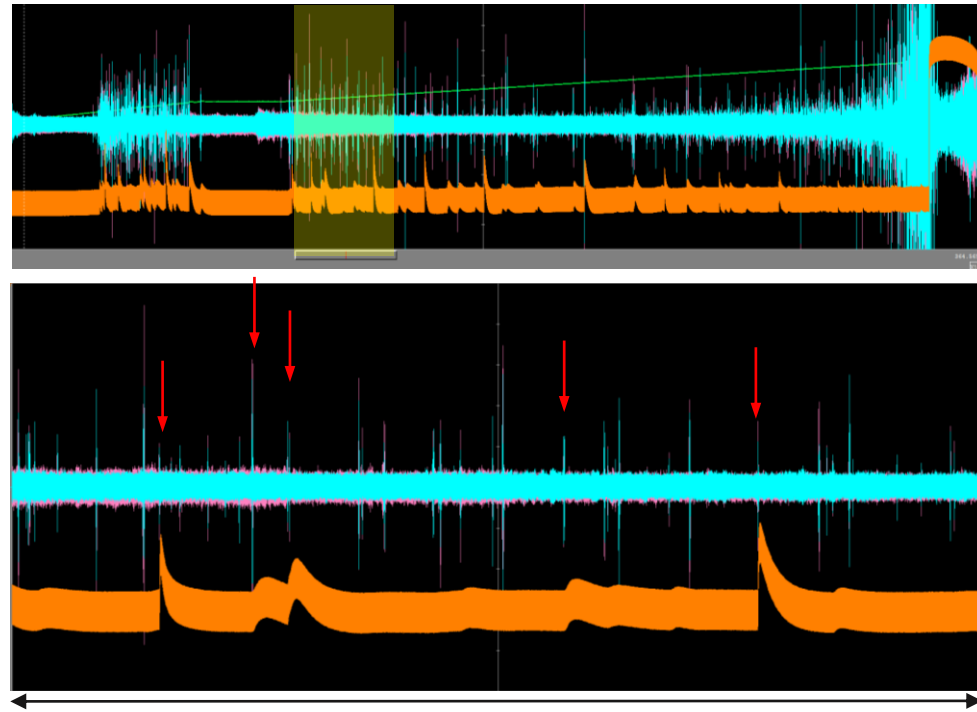
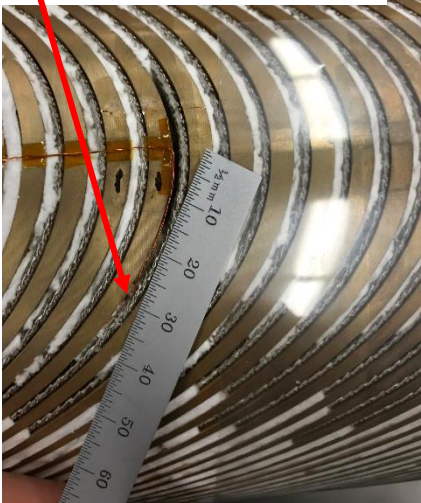


CCT Sub4 training and cumulative AE energy release

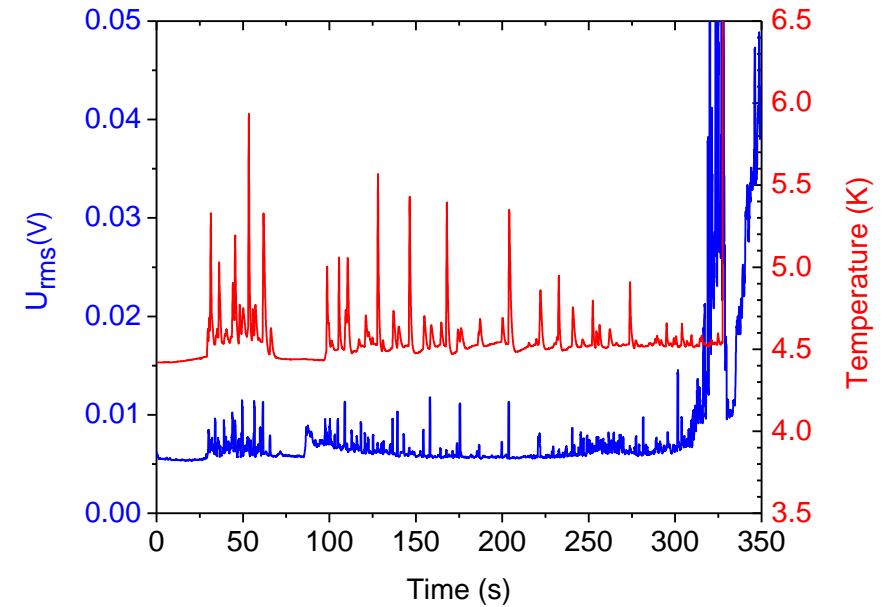


# Thermal and acoustic spikes are correlated

A thermometer of  $\sim 1 \text{ mm}^2$  size was installed directly in the cable groove, in the magnet outer layer, prior to impregnation

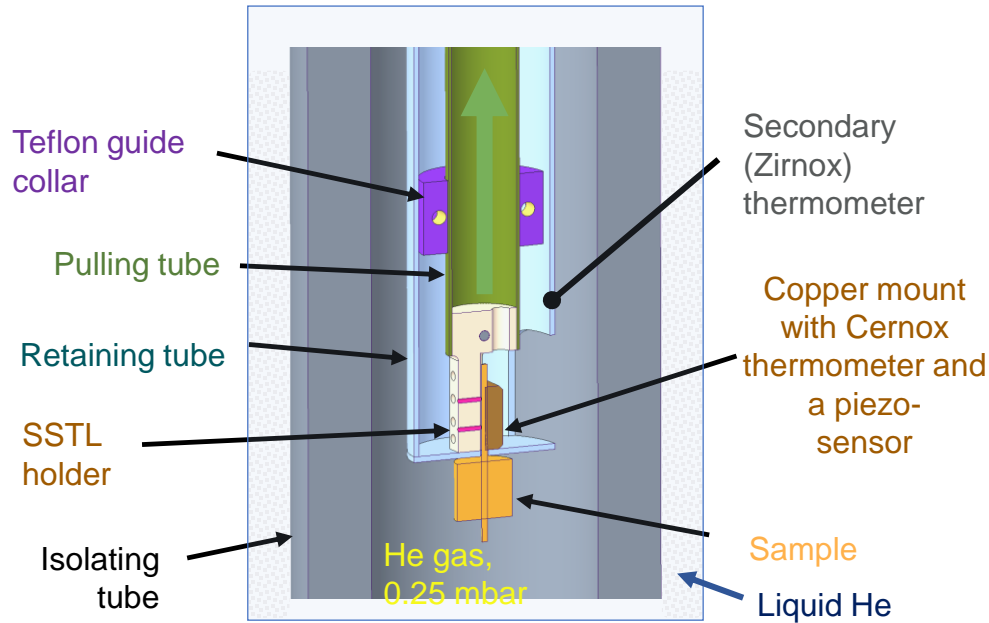


$\sim 36.5 \text{ s}$

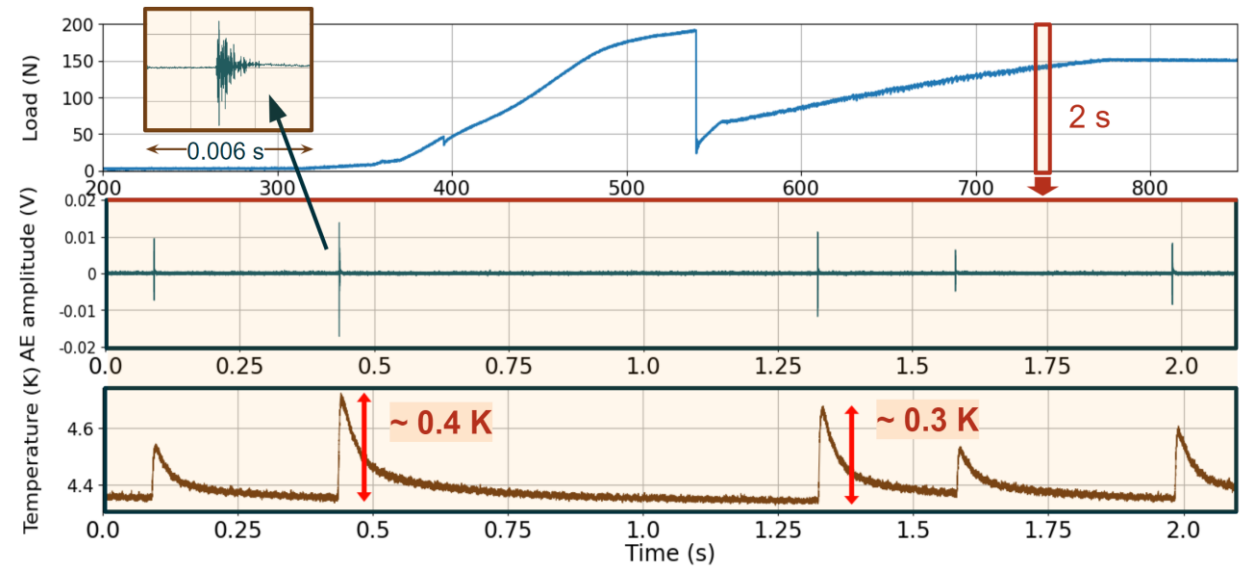
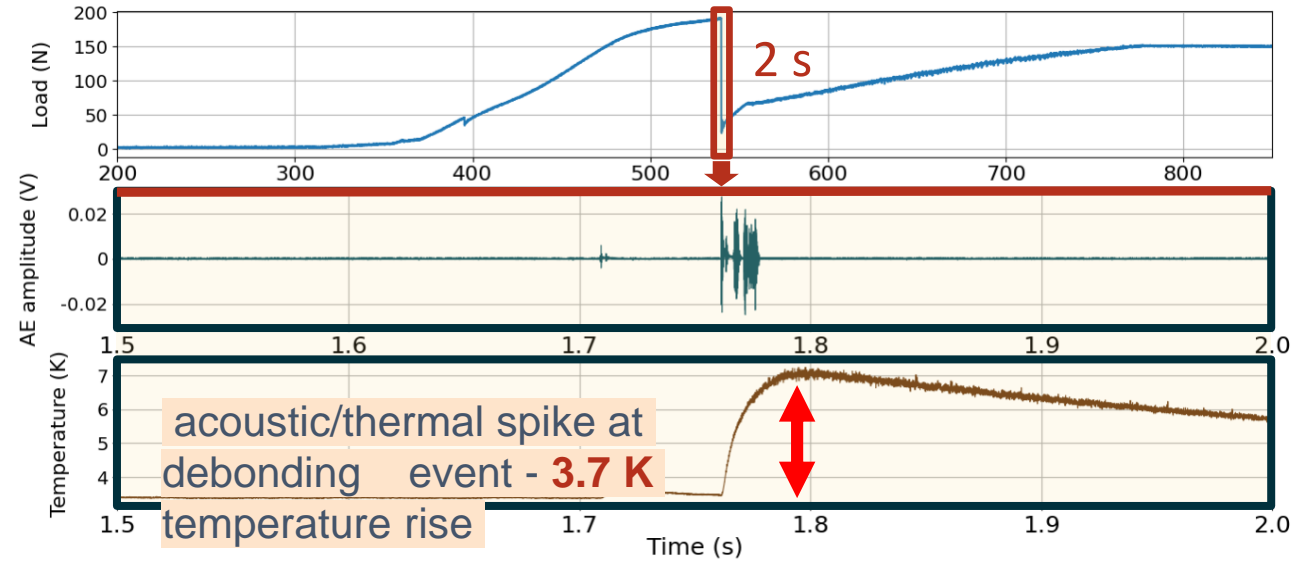


- Temperature spikes as high as 1 K are observed in the “cracking” regime. All of them are time-correlated with the acoustic events, and few also correlate with voltage spikes on the coils
- A minor ( $< 20 \text{ mK}$ ) gradual temperature rise, or none at all is seen in the “slip-stick” regime prior to quenching

# Acoustic emissions and temperature rise associated with the mechanical transients measured in a small-scale experiments

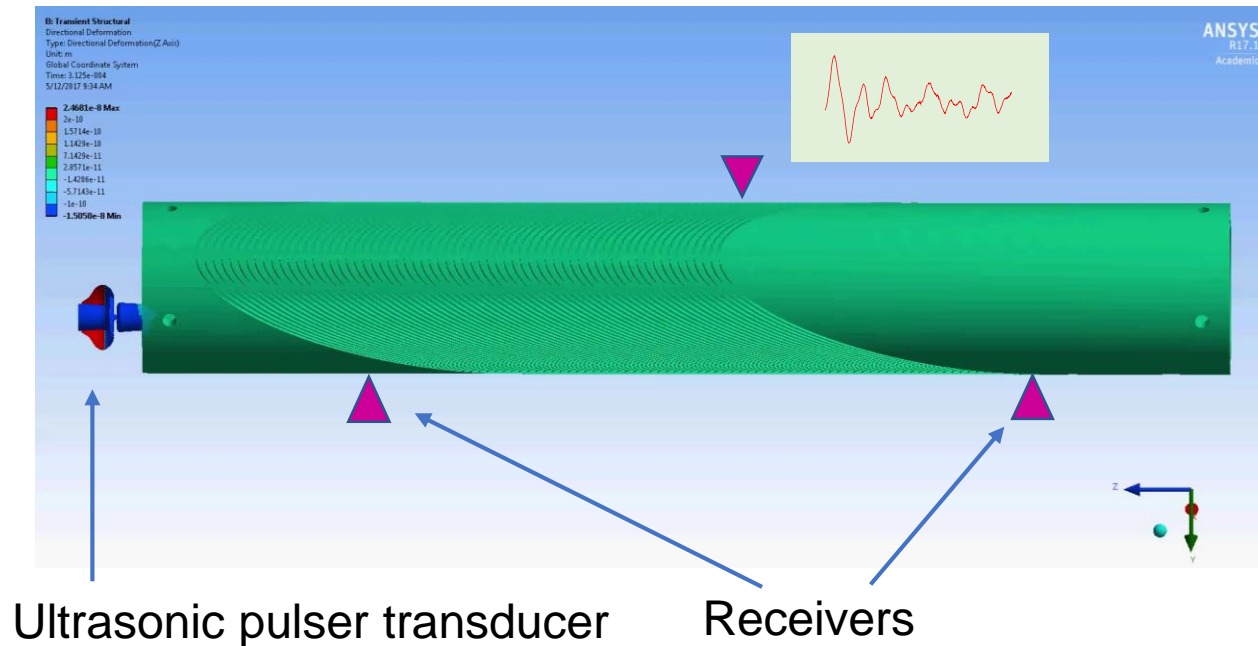


A. Saravanan et al., IEEE Trans. Appl. Supercond. 2025, 35, 4701205, [10.1109/TASC.2025.3526098](https://doi.org/10.1109/TASC.2025.3526098)



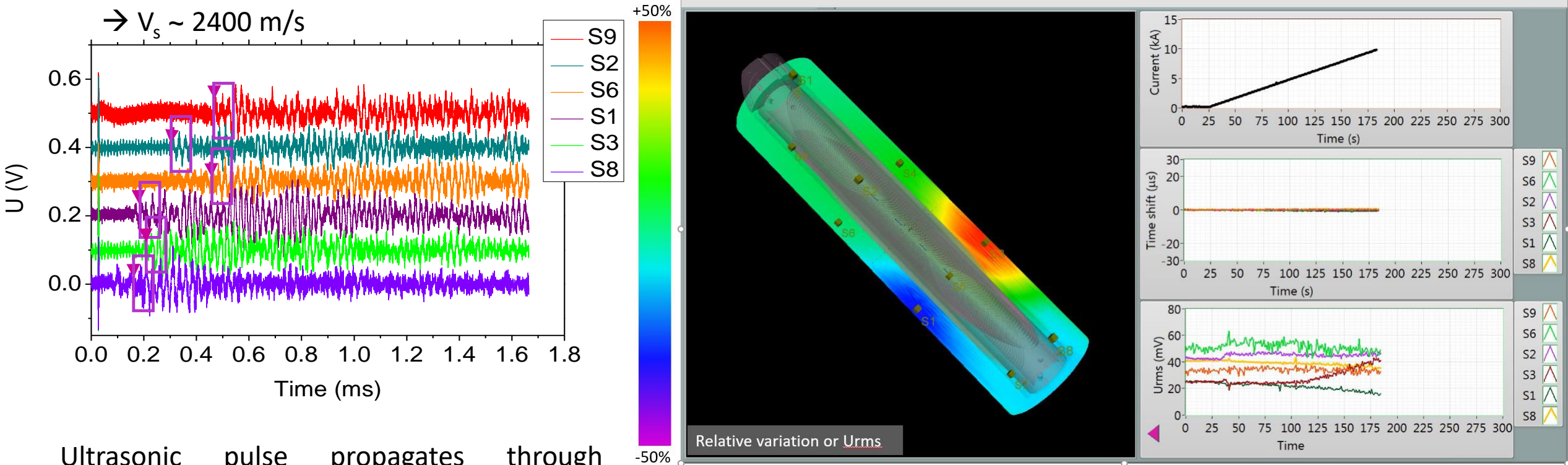
# Active monitoring of mechanical integrity

ANSYS simulation of transient deformation in the CCT mandrel upon pulsing a piezo-transducer



- Coil is pulsed using a piezo-transducer, and resulting perturbation is recorded by sensors distributed along the magnet
- The ring-down deformation  $x(t)$  at any location is uniquely defined by the magnet geometry, Young's moduli of the materials, and their mutual **interfaces**
- Acoustic wave reverberates multiple times thus allowing to **detect structural perturbation** anywhere in the magnet
- Technique is **non-invasive**, and be **adapted to existing magnet systems**

# Probing mechanical interfaces with pulsed acoustics



Ultrasonic pulse propagates through interfaces between the inner layer and outer layer -> mandrel of the magnet. When the magnet is energized, interfacial contact changes due to Lorentz forces on the coils

- As magnet deforms under stress, sensors S2 and S3 are seeing an improving mechanical contact between shell and inner / outer layers, while S1 is seeing a loss of mechanical contact.

M. Marchevsky, D. Arbelaez and S. Prestemon, "Structural Diagnostics of Superconducting Magnets Using Diffuse Field Ultrasound," in *IEEE Transactions on Applied Superconductivity*, vol. 30, no. 4, pp. 1-4, June 2020,



# Non-voltage quench detection for HTS



# Why non-voltage techniques are needed?

If the quench propagates very slowly, a hot spot may reach a high temperature while the voltage rise (proportional to the normal volume) will still be very small.. => a high risk of damaging the conductor.

A problem for HTS conductors, as there NZPV is 1-2 orders of magnitude slower than in LTS!

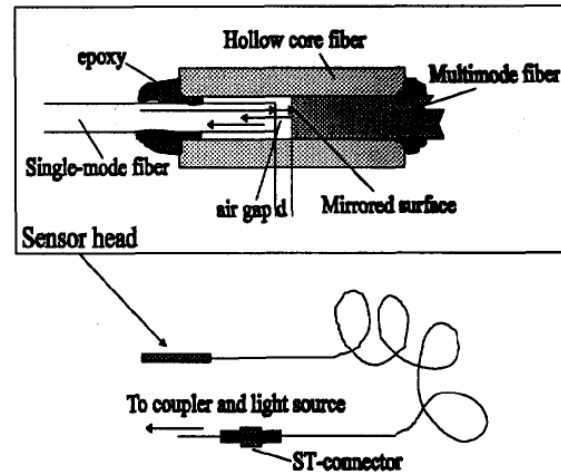
HTS magnets quench not on a “voltage criterion” but through a thermal runaway that occurs when heat is generated faster than removed. Voltage only gives “heat in” integrated over the conductor length... but no information on “heat out”

**Alternative: monitoring temperature variations**

# Optical techniques

**Optical sensing: based on detecting local stresses generated by a hot spot**

## Fiber-optic interferometer



J.M. van Oort, R.M. Scanlan and H.H.J ten Kate., “A Fiber-optic Strain Measurement and Quench Localization System for Use in Superconducting Accelerator Dipole Magnets”, *IEEE Trans. Appl. Supercond.* 5, 882 (1995)

**The sensitivity of the fiber optic sensors for absolute readout is in the order of 50 - 100 nm, which yields a strain resolution of the order of  $10 \times 10^{-6}$  in the longitudinal and radial direction. The pressure resolution in the transverse direction is in the order of 5 MPa.**

## Rayleigh scattering

W.K. Chan, G. Flanagan and J. Schwartz, “Spatial and temporal resolution requirements for quench detection in (RE)Ba<sub>2</sub>Cu<sub>3</sub>O<sub>x</sub> magnets using Rayleigh-scattering-based fiber optic distributed sensing”, *Supercond. Sci. Technol.* 26 105015 (2013).

## Fiber Bragg gratings (FBG)

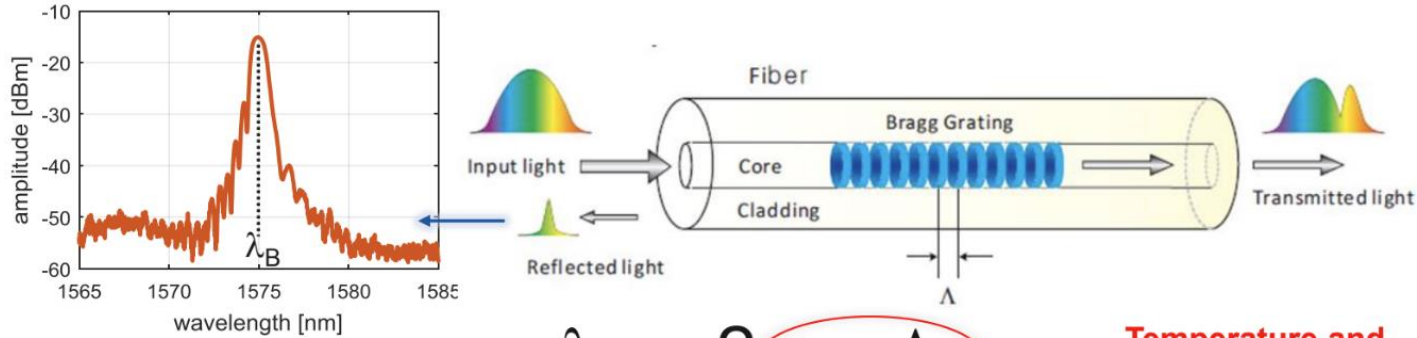
F. Hunte et al., “Fiber Bragg optical sensors for YBCO applications”, Proceedings of PAC09, Vancouver, BC, Canada

**Pro:** immune to EM interference. High sensitivity. Proven to work on small coils.

**Con:** requires co-winding optical fiber with the conductor + an increasingly powerful data processing for detecting quenches in long coils. Detection time is ~1s.

# Fiber Bragg Gratings for quench detection

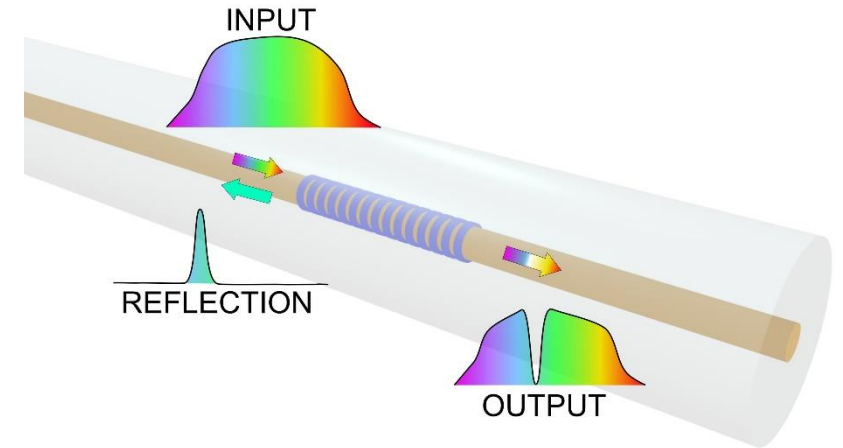
Acts as a band-stop **filter** passing all wavelengths that are not in resonance with the grating and reflecting wavelengths that satisfies the Bragg condition



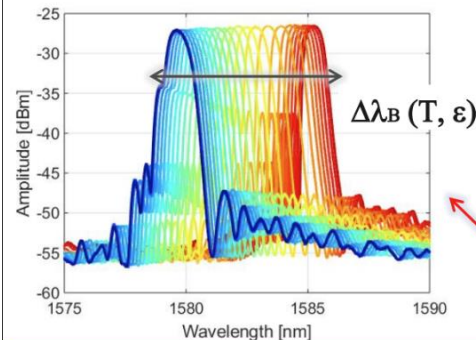
$$\lambda_B = 2 n_{\text{eff}} \Lambda$$

•  $n_{\text{eff}}$  = effective refractive index of the core  
 •  $\Lambda$  [nm] = grating period

Temperature and strain dependent



The FBG is sensitive to both temperature ( $T$ ) and strain ( $\epsilon$ ). **A change in these parameters leads to a shift** in the Bragg wavelength due to the effect they induce on both the refractive index  $n_{\text{eff}}(T, \epsilon)$  and the grating period  $\Lambda(T, \epsilon)$ .



$$\Delta\lambda_B = \frac{\partial\lambda}{\partial T} \Delta T + \frac{\partial\lambda}{\partial \epsilon} \Delta \epsilon$$

Sensors can be interrogated and then monitor the Bragg wavelength over time

*B. Castaldo et al., presentation at the IDSM01 workshop*

# Detecting heating through coil mechanical resonances

## Monitoring changes in vibrational frequency spectra and structural resonances due to local heating within the windings

- T. Ishigohka et al., “Method to detect a temperature rise in superconducting coils with piezoelectric sensors”, Appl. Phys. Lett. 43 (3), pp. 317-318 (1983)
- A. Ninomiya et al., “Quench detection of superconducting magnets using ultrasonic wave”, IEEE Trans. Magn. 25, v2 pp 1520-1523 (1989)
- T. Ishigohka et al., “Method to detect a temperature rise in superconducting coils with piezoelectric sensors”, Appl. Phys. Lett. 43, 317 (1983)
- A. Ninomiya et al., “Monitoring of a superconducting magnet using an ultrasonic technique”, Fusion Eng. Design 20, 305-309, (1993)

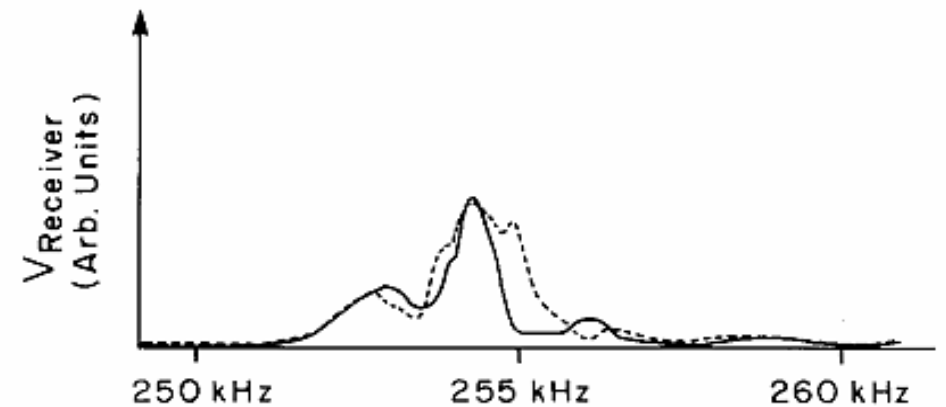


FIG. 3. Frequency spectra for the test coil immersed in a bath of liquid helium, with heater current zero (solid curve) and with heater current at 0.3 A (dotted curve).

**To be usable for quench detection, these techniques require mechanical modeling of the coil eigenfrequencies and transfer function that are experimentally validated prior to actual QD.**

# Detecting heating by measuring change in the sound propagation velocity

- Quench propagation velocity in HTS materials is < 50 mm/s at best circumstances, and typically much less (especially at LN2 temperature and below). This translates into a very localized hot spot that does not generate much resistive voltage => coil can burn before quench is detected...
- “Thermal” quench detection would solve that!

## What if we use the conductor itself as distributed temperature sensor?

Sound velocity:  $v = \sqrt{\frac{E}{\rho}}$ , where Young’s modulus E exhibits the strongest temperature dependence:  

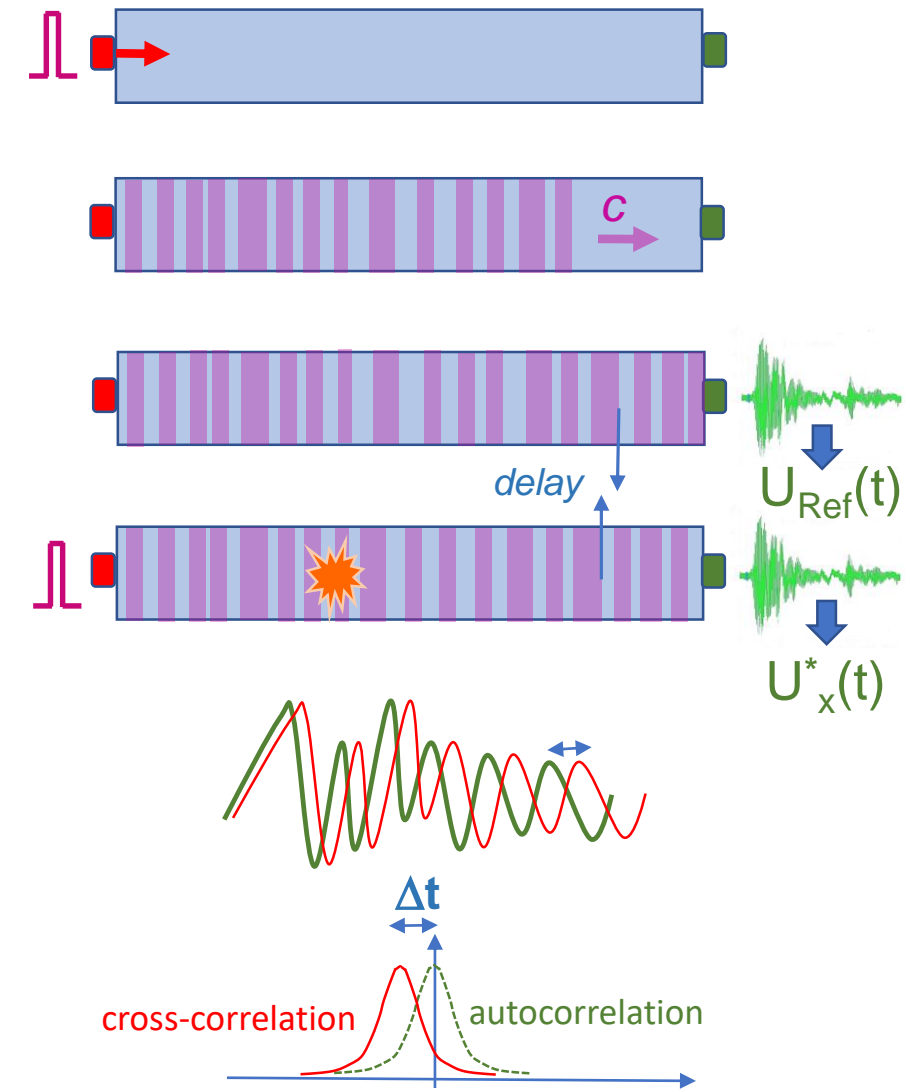
$$E(T) = E_0 - s/[e^{t/T} - 1]$$
 (s, t – adjustable parameters)

The E(T) dependence is **weak**: just ~1-10 ppm/K at 77 K and even less at lower temperatures. But it is still **measurable** using high-frequency ( $10^5$ - $10^6$  Hz) vibrational modes, and taking advantage of high (>100) mechanical Q-factor.

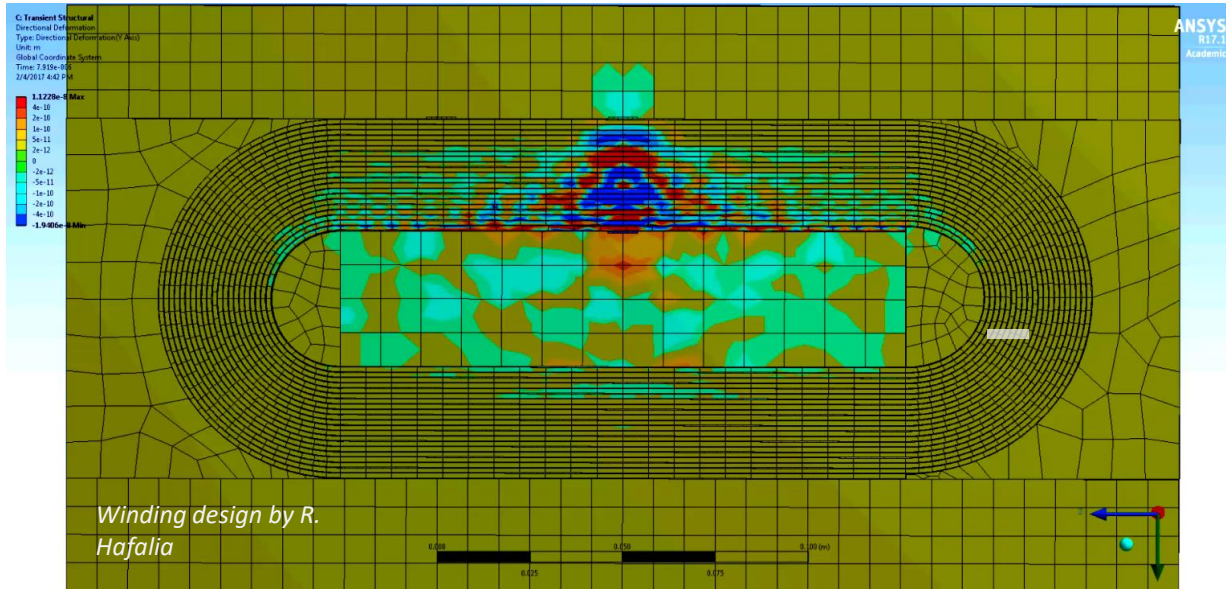
We do it by monitoring a **transient acoustic response**

# Ultrasonic thermometry principle

1. A body is **pulsed** by a sender ultrasonic transducer
2. A “ring-down” transient waveform propagates and reverberates multiple times
3. Transient oscillation is **acquired** by a receiver transducer; and stored as “reference”  $U_{\text{Ref}}(t)$ . Its shape is **uniquely defined** by the body geometry, density and elastic modulus  $E(T)$
4. Pulsing and transient acquisitions are repeated periodically; every new transient  $U_x(t)$  is compared to  $U_{\text{Ref}}(t)$  using cross-correlation:  $A(\Delta t) = U_x(t+\Delta t) * U_{\text{Ref}}(t)$ . The time shift  $\Delta t$  yielding the **maximal cross-correlation** is calculated for every new pulse
5. When a hot spot develops,  $E(T)$  decreases locally, delaying the wave passing through it. This proportionally increases  $\Delta t$ .

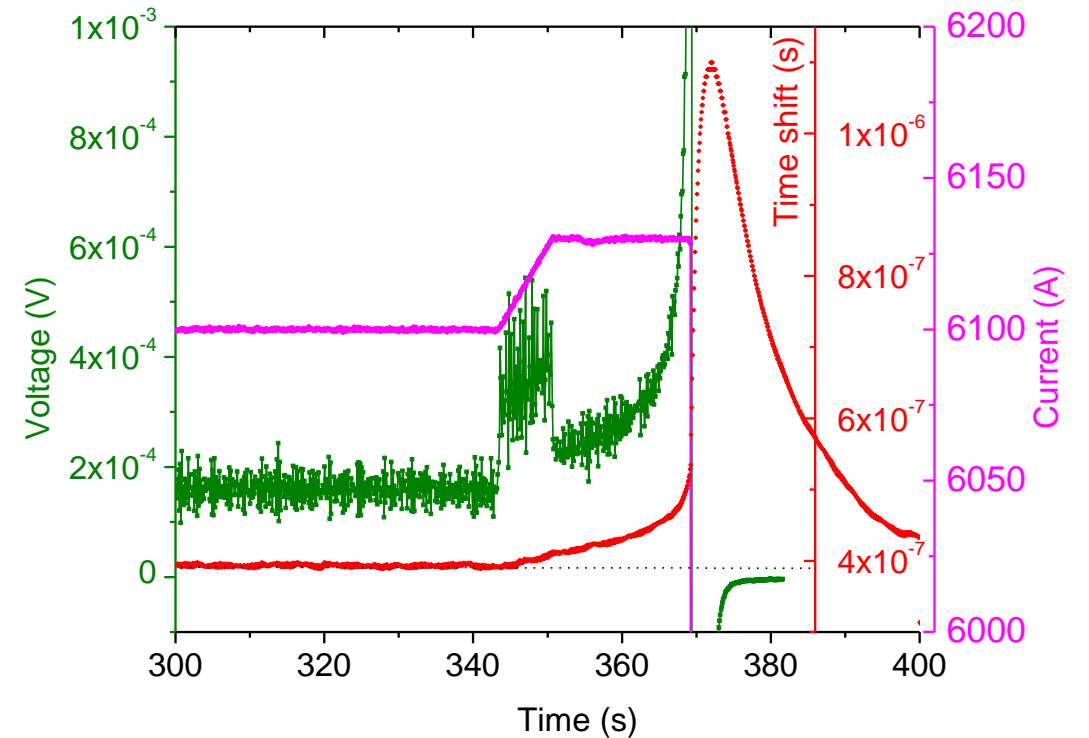


# Acoustic quench detection in Bi-2212 HTS coil



- Flat coil model: PET-insulated (0.2 mm thick) stainless tape (1.25 mm thick), stainless structure.
- Piezo-transducer is installed at the interface between central island and the first pole turn; pulsed with a 0.2  $\mu\text{s}$  duration pulse; and displacement along “y” is calculated with 0.1  $\mu\text{s}$  time step.

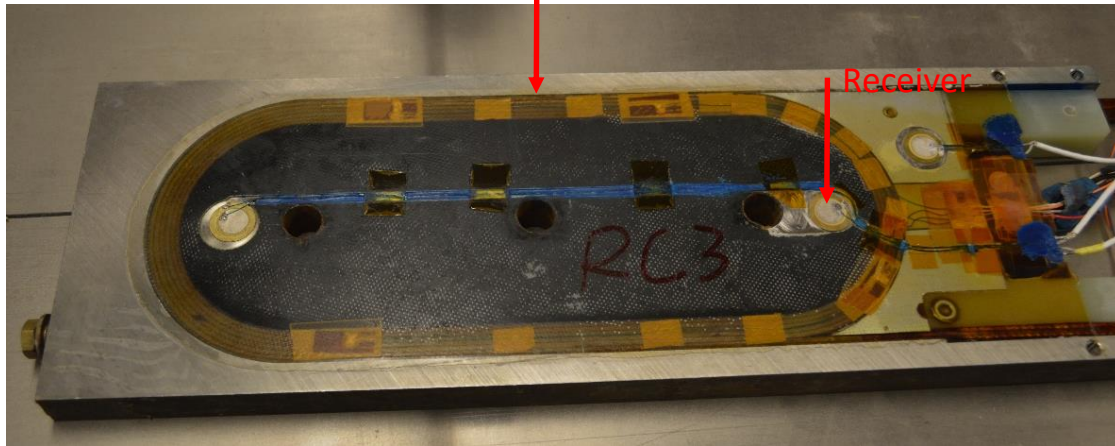
Experiment at 4.2 K. Current ramp stopped at 6100 A (stable) and then increased by 30 A (quenching)



Bi-2212 coil RC3

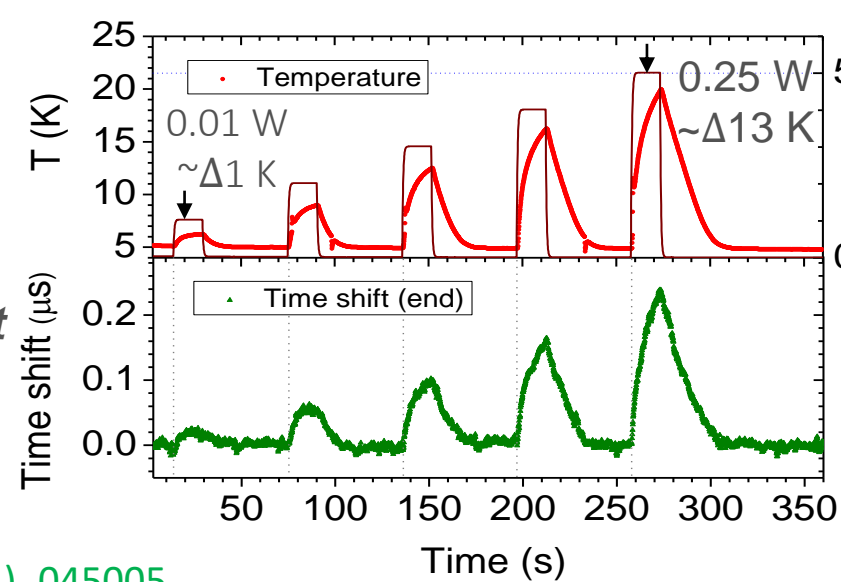
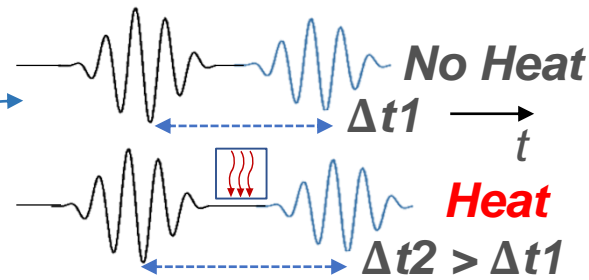
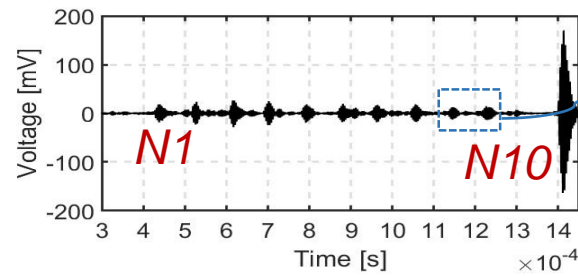
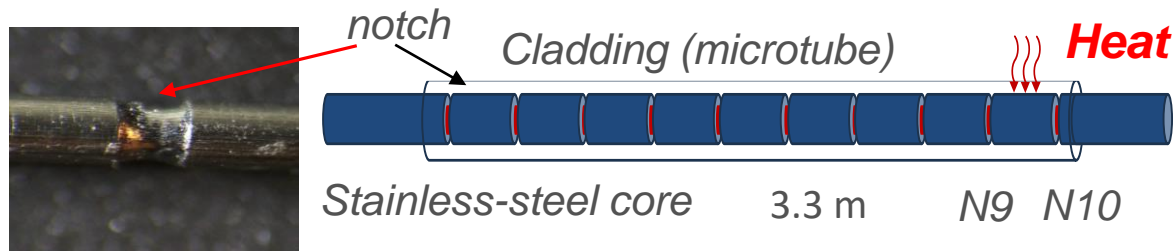
Pulser embedded in the winding

Receiver



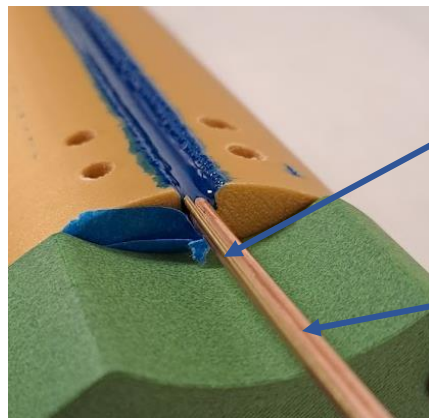
K. Zhang, T. Shen

# Ultrasonic waveguides enable distributed temperature sensing, can be integrated in an HTS coil



Time shift is detectable at  $\Delta T = 1\text{K}$  and heater power of 0.01 W.

M. Marchevsky and S. Prestemon, 2023, *Supercond. Sci. Technol.* 36(4), 045005

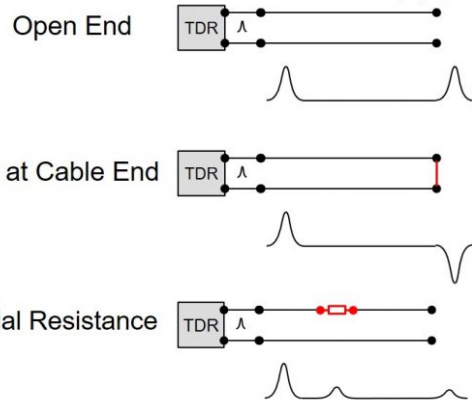


Ultrasonic waveguide  
CORC cable (mock-up)

D. Cuneo, J.L Rudeiros-Fernandez



## TDR pulse response



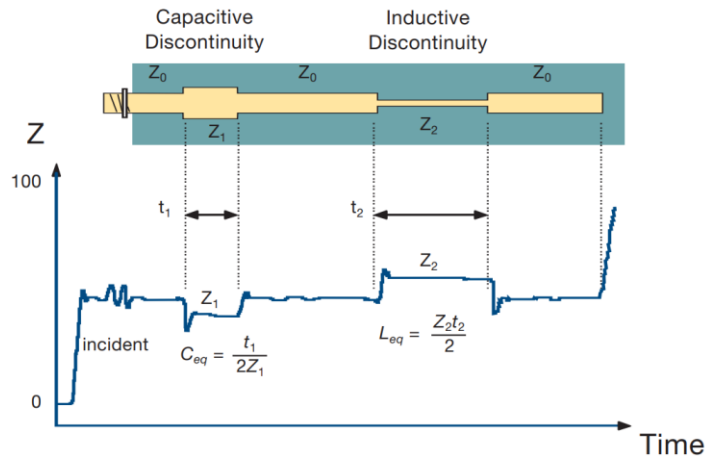
$$S_{11}(\omega) = X(\omega) + jY(\omega)$$



$$U(t) = \frac{1}{N} \sum_{i=0}^{N-1} w_i S_{11}(\omega_i) e^{j\omega_i t}$$

$$w_i = \sum_{k=0}^{m-1} (-1)^k \cos\left(\frac{2\pi i k}{N}\right)$$

## TDR step response

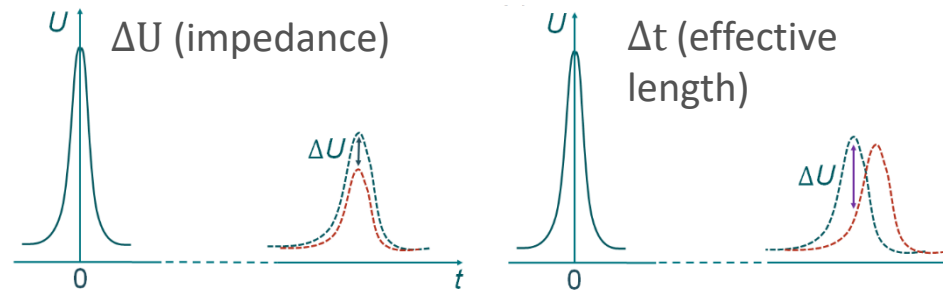


## Coaxial cable

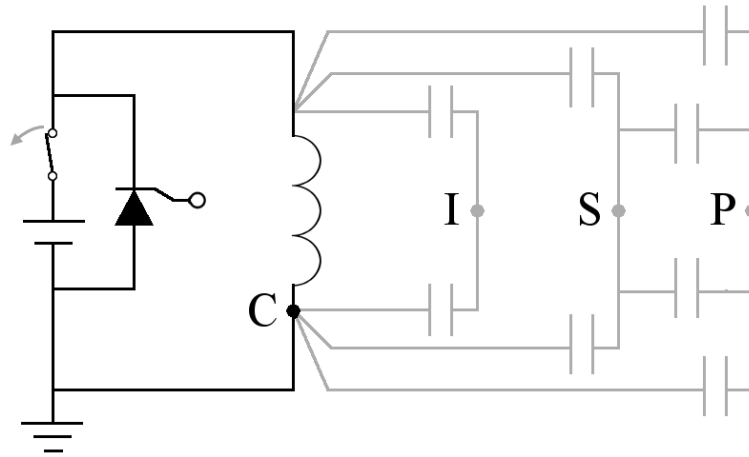
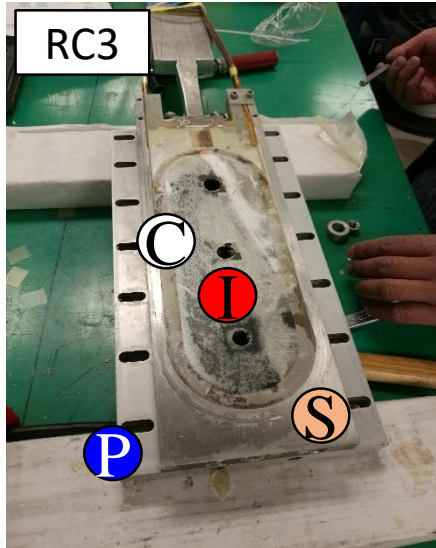


$$Z = \sqrt{\frac{L}{C}} = \frac{1}{2\pi} \sqrt{\frac{\mu_0}{\epsilon_0 \epsilon_r(T)}} \ln\left(\frac{b}{a}\right) \quad v = \frac{c}{\sqrt{\epsilon_r(T)}}$$

M. Marchevsky *et al.*,  
*Trans. Appl. Supercond.*,  
 2023, **33**, 9000206.



- Senses local heating through the change of RF impedance and propagation velocity due to heating-induced variation of the electrical permittivity of the insulator



$$C = \epsilon_0 \epsilon_r S/s$$

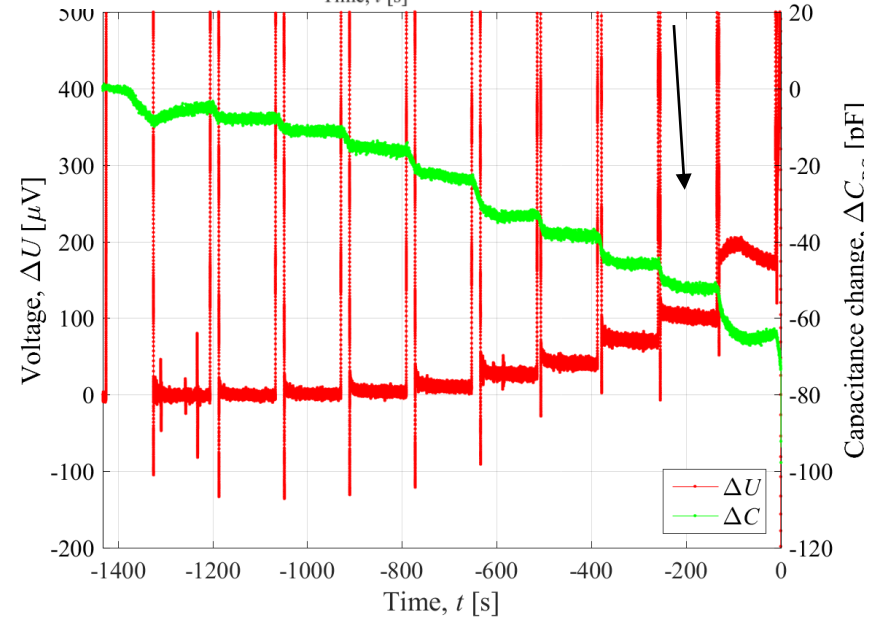
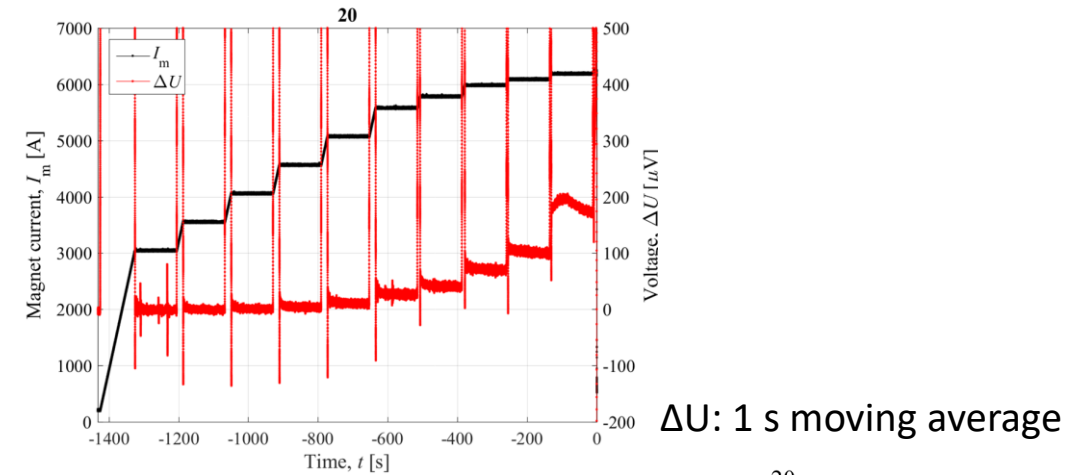
$\epsilon_0 = 8.854 \cdot 10^{-12} \text{ Fm}^{-1}$   
 $\epsilon_r$  rel permittivity  
 $S$  contact surface  
 $s$  distance

Stray capacitance can be measured between any metallic component electrically insulated from the others

The mechanism leading to stray capacitance change just before quench is the decrease of cryogen fluid's electrical permittivity  $\epsilon_r$  when the phase change occurs.

This happens when the fluid impregnating the insulation boils off.

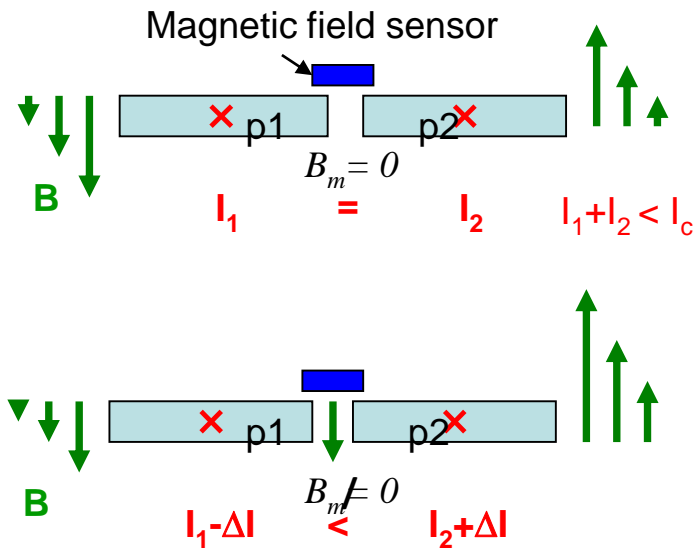
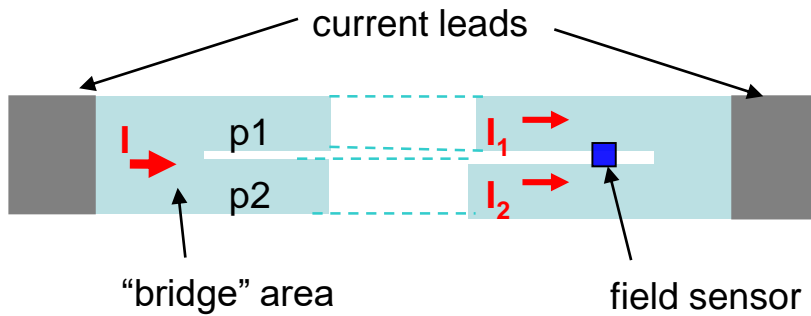
“Quench Detection Utilizing Stray Capacitances”, E. Ravaioli, et al., IEEE Trans. Appl. Supercond. 28, 4702805 (2018)



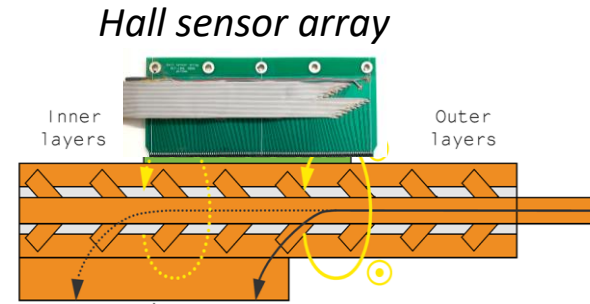
Measured magnet voltage does not include voltage drop across the splices

# Hall sensor-based diagnostics can be superior to voltage for low inductance or non-ramping magnet applications

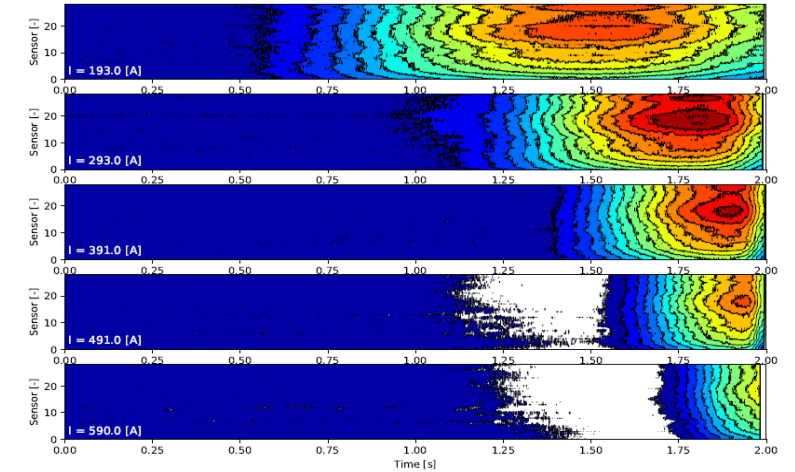
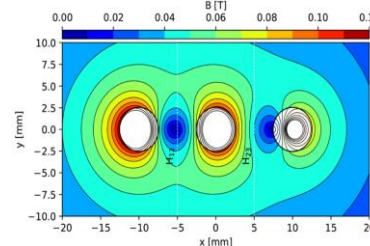
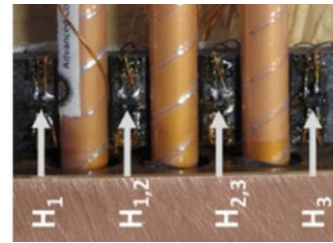
Splitting conductor over components that are joined at terminations with low-resistance joints enables probing resistance onset through current re-distribution.



- The technique can sense heating at the very onset of resistance,  $I < I_c$  (!)



Integration of a Hall array into an HTS CORC<sup>®</sup> cable terminal



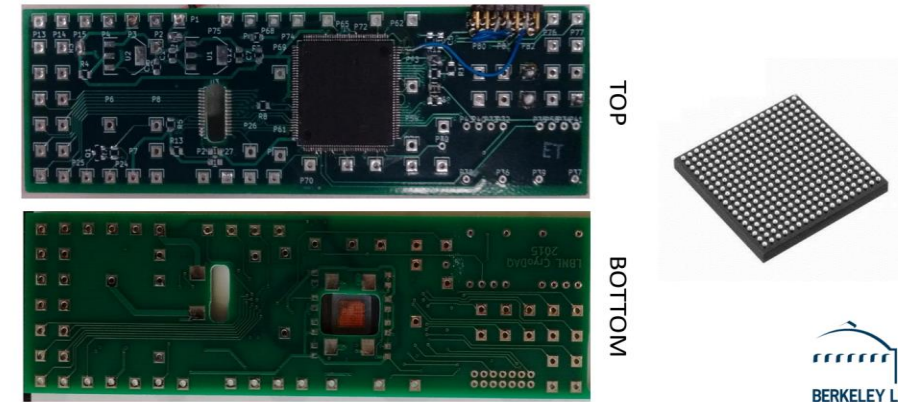
Field variation measured along the terminal as resistance develops in the cable outer layer

Hall sensor integration with a CORC<sup>®</sup>-based triplet conductor

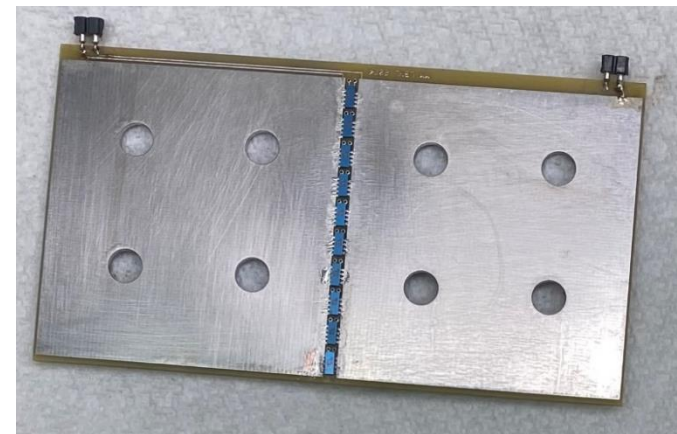
M. Marchevsky *et al.*, *Supercond. Sci. Technol.* 2010, **23** 034016  
 R. Teyber, *et al.*, *Supercond. Sci. Technol.*, 2020, **33** 095009  
 J. Weiss *et al.*, *Supercond. Sci. Technol.* 33, 105011, (2020)  
 R. Teyber *et al.*, *Sci. Rep.*, 2022, **12**, 22503.

# Cryogenic electronics

- Cryogenic amplifiers and quench detectors
- Cryogenic FPGA and data processing for diagnostic instrumentation
- Cryogenic current control for quench protection and magnet powering



Cryo FPGA board (M. Turqueti, LBNL)



Cryogenic MOSFETs



Thank you!